

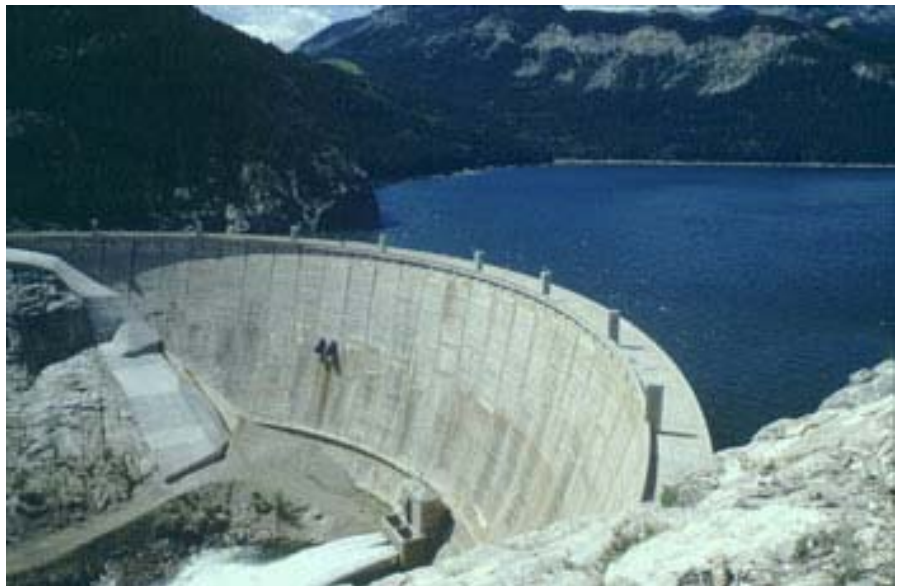
RECLAMATION

Managing Water in the West

Hydraulic Laboratory Report HL-2006-02

Hydraulic Investigations of the Erosion Potential of Flows Overtopping Gibson Dam

Sun River Project, Montana
Great Plains Region



U.S. Department of the Interior
Bureau of Reclamation
Technical Service Center
Water Resources Research Laboratory
Denver, Colorado

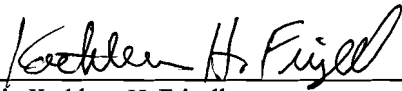
April 2006

REPORT DOCUMENTATION PAGE				Form Approved OMB No. 0704-0188	
<p>The public reporting burden for this collection of information is estimated to average 1 hour per response, including the time for reviewing instructions, searching existing data sources, gathering and maintaining the data needed, and completing and reviewing the collection of information. Send comments regarding this burden estimate or any other aspect of this collection of information, including suggestions for reducing the burden, to Department of Defense, Washington Headquarters Services, Directorate for Information Operations and Reports (0704-0188), 1215 Jefferson Davis Highway, Suite 1204, Arlington, VA 22202-4302. Respondents should be aware that notwithstanding any other provision of law, no person shall be subject to any penalty for failing to comply with a collection of information if it does not display a currently valid OMB control number.</p> <p>PLEASE DO NOT RETURN YOUR FORM TO THE ABOVE ADDRESS.</p>					
1. REPORT DATE (DD-MM-YYYY) April 2006		2. REPORT TYPE Technical		3. DATES COVERED (From - To) December-April 2006	
4. TITLE AND SUBTITLE Hydraulic Investigations of the Erosion Potential of Flows Overtopping Gibson Dam Sun River Project, Montana Great Plains Region				5a. CONTRACT NUMBER	
				5b. GRANT NUMBER	
				5c. PROGRAM ELEMENT NUMBER	
6. AUTHOR(S) Kathleen H. Frizell				5d. PROJECT NUMBER	
				5e. TASK NUMBER	
				5f. WORK UNIT NUMBER	
7. PERFORMING ORGANIZATION NAME(S) AND ADDRESS(ES) Bureau of Reclamation Technical Service Center Water Resources Research Laboratory Denver, Colorado				8. PERFORMING ORGANIZATION REPORT NUMBER HL-2006-02	
9. SPONSORING/MONITORING AGENCY NAME(S) AND ADDRESS(ES) U.S. Department of the Interior Bureau of Reclamation PO Box 25007 Denver, CO 80225				10. SPONSOR/MONITOR'S ACRONYM(S)	
				11. SPONSOR/MONITOR'S REPORT NUMBER(S)	
12. DISTRIBUTION/AVAILABILITY STATEMENT National Technical Information Service, 5285 Port Royal Road, Springfield, VA 22161 http://www.ntis.gov					
13. SUPPLEMENTARY NOTES					
14. ABSTRACT This report discusses the results of the hydraulic investigation of the potential overtopping of Gibson Dam. Overtopping protection has been constructed on both the right and left abutments at Gibson Dam since 1984. This report documents the hydraulic investigations that were completed to determine if the jet from the new 2005 Probable Maximum Flood would impact on the extent of the existing overtopping protection. The analysis techniques used to determine the overtopping jet characteristics and the results from the analysis are provided. The jet impacts beyond the protection on the right abutment between El. 4710 and 4650. The stream power density in the flow was also determined at various impact locations, both on and off the right abutment protection, to provide geotechnical engineers the information needed to determine if further protection is needed based upon the quality of the rock or the concrete repairs.					
15. SUBJECT TERMS concrete dam overtopping, jet trajectory, hydraulic investigations, dam abutment protection, stream power, Gibson Dam, Sun River Project, Montana					
16. SECURITY CLASSIFICATION OF:			17. LIMITATION OF ABSTRACT	18. NUMBER OF PAGES	19a. NAME OF RESPONSIBLE PERSON
a. REPORT	b. ABSTRACT	a. THIS PAGE			Clifford A. Pugh
UL	UL	UL	SAR	43	19b. TELEPHONE NUMBER (Include area code) 303-445-2151

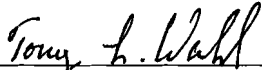
Hydraulic Laboratory Report HL-2006-02

Hydraulic Investigations of the Erosion Potential of Flows Overtopping Gibson Dam

Sun River Project, Montana
Great Plains Region



Prepared: Kathleen H. Frizell
Hydraulic Engineer, Water Resources Research Laboratory, D-8560



Technical Approval: Tony L. Wahl, P.E.
Hydraulic Engineer, Water Resources Research Laboratory Group, D-8560



Peer Review: Clifford A. Pugh, P.E. Date 4-12-06
Hydraulic Engineer, Water Resources Research Laboratory Group, D-8560

REVISIONS					
Date	Description	Prepared	Checked	Technical Approval	Peer Review



U.S. Department of the Interior
Bureau of Reclamation
Technical Service Center
Water Resources Research Laboratory
Denver, Colorado

April 2006

Mission Statements

The mission of the Department of the Interior is to protect and provide access to our Nation's natural and cultural heritage and honor our trust responsibilities to Indian Tribes and our commitments to island communities.

The mission of the Bureau of Reclamation is to manage, develop, and protect water and related resources in an environmentally and economically sound manner in the interest of the American public.

Acknowledgments

This project was requested by John Steighner, Geotechnical Engineering Group 2, D-8312, to assist with the Corrective Action Study for Gibson Dam. Elisabeth Cohen, Waterways and Concrete Dams Group, D-8130, provided invaluable reference material regarding analysis techniques. Rudy Campbell, Water Resources Research Laboratory, D-8560, provided assistance with the ACAD presentation of the results. Technical peer review was provided by Tony L. Wahl, Water Resources Research Laboratory, D-8560.

Hydraulic Laboratory Reports

The Hydraulic Laboratory Report series is produced by the Bureau of Reclamation's Water Resources Research Laboratory (Mail Code D-8560), PO Box 25007, Denver, Colorado 80225-0007. At the time of publication, this report was also made available online at http://www.usbr.gov/pmts/hydraulics_lab/pubs/HL/HL-2006-02.pdf

Disclaimer

No warranty is expressed or implied regarding the usefulness or completeness of the information contained in this report. References to commercial products do not imply endorsement by the Bureau of Reclamation and may not be used for advertising or promotional purposes.

TABLE OF CONTENTS

I.	Executive Summary	1
II.	Introduction	3
	A. Purpose.....	3
	B. Background.....	3
III.	Site Geology	5
IV.	Site History.....	7
V.	Hydrologic Issues.....	10
VI.	Flood Routings	10
VII.	Freeboard	13
VIII.	Tailwater Information	14
IX.	Hydraulic Loading.....	15
	A. Definitions.....	16
	B. Trajectory Calculations.....	18
	1. Jet Spread in the Free Fall.....	22
	2. Jet Break Up Length in Free Fall.....	24
	a) Jet Trajectories for Various Overtopping Flows.....	25
	C. Jet Plunge Pool Characteristics.....	28
	D. Stream Power	32
X.	Recommendations	35
XI.	References	35

Appendix A - Drawings

Appendix B – Sensitivity of the jet trajectory to the “K” factor in the equation of motion

FIGURES

Figure 1. - Gibson Dam downstream right abutment before construction of the concrete cap.....	6
Figure 2. - Gibson Dam downstream right abutment after installation of the concrete cap and rock bolts.....	9
Figure 3. - Gibson Dam frequency flood routing results for the various storm events, initial reservoir elevations and spillway gate operations.....	13
Figure 4. - Result of a preliminary tailwater study for the toe of Gibson Dam under the PMF. The maximum tailwater occurs about 38 hours into the routing with an elevation of 4669.9 ft.....	15
Figure 5. – Free jets (a) overtopping a dam, (b) issuing from an orifice through a dam, (c) definition sketch for parameters of a free falling jet. (Bollaert, 2002).	17
Figure 6. - Sectional view of the final trajectory profile for the PMF for Gibson Dam through dam section A-A aligned with the river channel.....	20
Figure 7. - Footprint of the trajectory with no spread of the jet for the PMF overtopping at Gibson Dam. Note the location of the footprint extends beyond the right	

abutment protection between contour elevations 4660 and 4710. The tailwater for the PMF is shown on the plan view in blue at El. 4670..... 21

Figure 8. - Sectional view of predicted trajectories for various frequency overtopping flood events at Gibson Dam..... 27

Figure 9. - Jet diffusion in a plunge pool for single-phase and two-phase shear layers: a) submerged jet ; b) almost laminar plunging jet; c) smooth turbulent plunging jet; d) highly turbulent plunging jet (Ervine and Falvey, 1987)..... 28

Figure 10. - Stream power versus erodibility index for the 1964 overtopping event at Gibson Dam. 33

Figure 11. - Relationship between stream power and erodibility index for the PMF overtopping of Gibson Dam. Estimates shown include stream power above and below the tailwater. 35

Figure 12. - Plan view of Gibson Dam showing the morning-glory spillway near the left abutment, the outlet works near the center of the river channel, and the overtopping protection added to the abutments in 1982. (This is a portion of drawing 28-D-822.) 39

Figure 13. - Sections through Gibson Dam showing the top of dam and the overall extent of the dam section. 40

Figure 14. - Comparison of jet trajectories with the assumed K factor for the PMF overtopping of Gibson Dam..... 43

TABLES

Table 1. - General storm rain-on-snow frequency floods for Gibson Dam. 10

Table 2. - Summary of frequency flood routing results for Gibson Dam..... 12

Table 3. - Summary of frequency flood routing results for events with freeboard on the parapet wall. 14

Table 4. - Table of turbulence intensities for free falling jets Bolleart (2002). 23

Table 5. - Free-falling jet characteristics for the PMF overtopping at Gibson Dam. 23

Table 6. - Table of trajectory results for various frequency flood events with x (horizontal) and y (vertical) distances and elevations from the downstream parapet wall..... 26

Table 7. - Jet characteristics for the PMF overtopping of Gibson Dam including both the free-falling jet and the jet below the tailwater. 30

Table 8. - Estimated erodibility indices and critical stream power values for the surface downstream from Gibson Dam..... 33

Table 9. - Table of computed jet trajectories for various K values for the PMF overtopping of Gibson Dam..... 42

I. Executive Summary

This report describes the investigation into the location of the jet impingement during the potential PMF overtopping of Gibson Dam. The investigation used the latest technology available to define the jet trajectory and the impact zone and determined the energy available at various impact elevations. Information is provided so that a decision may be made regarding whether or not the existing concrete protection on the right abutment of the dam is adequate. Further study may be required if it is determined that the results presented indicate unacceptable risk for the dam.

Gibson Dam and Reservoir are located on the North Fork of the Sun River about 24 miles northwest of Augusta, Montana. The dam was designed by the Bureau of Reclamation (Reclamation) and constructed by the Utah Construction Company in 1929. The dam is operated and maintained by the Greenfields Irrigation District with oversight by Reclamation's Montana Area Office (MTAO) in Billings, Montana. The Irrigation District normally operates the dam to maximize reservoir storage for distribution of water during the irrigation season. The reservoir has a storage capacity of about 96,477 acre-feet at the top of the active conservation pool, elevation 4724.0.

Gibson Dam is a massive concrete arch structure with a structural height of 199 feet and a hydraulic height of 195 feet. The crest of the dam is 15 feet wide and approximately 960 feet long at elevation 4725.5. Parapet walls are located on both the upstream and downstream edges of the crest, with the top of the parapets at elevation 4729.0. The spillway is located through the left abutment and has a funnel-shaped (or morning glory type) drop inlet just upstream from the north end of the dam. The original free-flow inlet crest was modified in 1938, and six 34-foot-wide by 12-foot-high radial gates were installed at the inlet crest. The spillway inlet crest is at elevation 4712.0. The outlet works is located near the center of the arch dam. It consists of a trashrack structure, two 72-inch-diameter semi steel-lined conduits through the base of the dam, two 5-foot-square high pressure emergency slide gates, and two 60-inch regulating jet-flow gates in a concrete gate house at the downstream toe of the dam. The jet-flow gates were installed in 1972 to replace the two needle valves installed during original construction. Plan and section views of the dam are shown in Appendix A on figures 12 and 13.

After an overtopping event in 1964, modifications to Gibson Dam were completed in 1982 to permit safe overtopping of the dam of up to 12 feet over the parapet walls. These modifications included excavation of unstable rock on both abutments just downstream from the dam, installation of groutable rock bolts to reinforce and stabilize jointed rock in the abutments, and placement of concrete caps on both abutments to help protect them during overtopping. The concrete cap is very extensive over the right abutment as shown on figure 2. The cap on the right abutment was designed with a minimum thickness of 2.5 ft but has no waterstops between slabs and no drainage provided.

The flood routings recently developed for Gibson Dam [4] are summarized in this document and were used in evaluation of the overtopping event.

The jet trajectory characteristics both through the air and in the plunge pool are summarized in table 7. The footprint of the jet from the PMF is shown on figure 7 in the body of the report. The tailwater for the PMF is at El. 4670. The footprint of the jet impinges on the right abutment beyond the protective concrete slab between Els. 4710 and 4660. The stream power at the impingement locations is between 88 and 131 HP/ft² (706 and 1048 kW/m²), respectively. The stream power is a maximum of 154 HP/ft² (1238 kW/m²) for the free-falling jet at El. 4670 where the jet would impact the tailwater. In the tailwater, the core of the jet is fully dissipated after plunging 10 ft or at El. 4660. The outer edge of the jet also spreads and the footprint increases, thus decreasing the power per square foot in the pool.

The plot of the relationship between the erodibility index and the stream power indicates that erosion would be expected in the more fractured rock abutment areas under the PMF. Stream power estimates indicate that scour could occur for impingement on the concrete surfaces below elevation 4708.5 for the low strength estimate and below elevation 4697.8 for the higher strength estimate. Stream power estimates indicate that scour could occur for impingement on the hard rock foundation estimated to be of lower strength below elevation 4715.8. Stream power estimates for the higher strength hard rock foundation indicate that scour should not occur. Figure 11 shows the plot of the stream power and erodibility for evaluation.

The trajectory for the PMF shows impingement beyond the concrete slab protection on the right abutment. Therefore, the trajectory calculations were requested for smaller frequency flood events. The results are shown in table 7 and figure 8. Preliminary examination shows that events up to the 100,000 year event will fall onto the protection and events exceeding the 100,000 year event again impinge beyond the protection.

Further assessment of stream power at lesser frequency events might be necessary to determine if selection of another design flood event is acceptable. In addition, the erodibility of the rock and concrete materials might be reassessed.

II. Introduction

A. Purpose

The purpose of this report is to document the results of the hydraulic investigations regarding overtopping of the dam and impingement on the dam rock abutments or previous concrete repairs for Gibson Dam, Montana [1]. In addition, the stream power per unit area or the energy per unit area throughout the range of impact elevations will be determined.

The May 2004 Issue Evaluation Report of Findings [1] made Recommendation 2004-SOD-A: “Initiate corrective action studies for stabilizing the right abutment.” In further discussion of 2004-SOD-A, the December 2004 Comprehensive Facility Review (CFR) [2] mentions that an evaluation of hydrodynamic loading should be part of the corrective action study (CAS) efforts for Gibson Dam in identifying measures to stabilize the right abutment. The Hydrologic Hazard Curve [3] and new Probable Maximum Flood were completed in November 2005 in the draft TM entitled “Gibson Dam Frequency Flood Routings for Corrective Action Study” [4] as per Safety of Dams recommendation 2004-SOD-B. The hydrodynamic loading is a necessary component to stabilizing the abutments at Gibson Dam. This information was used to determine the amount and duration of overtopping in the assessment of the location and intensity of the hydraulic loading at the dam being evaluated in this report.

The purpose of this report is to address a portion of SOD Recommendation 2004-SOD-A resulting from the CFR as a portion of the CAS.

2004-SOD-A – Proceed with corrective actions to reduce seismic risks on the right abutment. Consider installation of rock reinforcement to precede installation of foundation drains recommended by 2000-SOD-A. (DSIS data base, 10/29/2004)

Discussion: A finding of the CFR performed in December 2004 was to develop a new Probable Maximum Flood for Gibson Dam and to use this updated flood to evaluate the hydrodynamic loading on the dam abutments.

This report describes the results from the analysis for the overtopping of Gibson Dam based upon the 2005 flood event and knowledge of the existing abutment geometry and protection.

B. Background

Gibson Dam and Reservoir are located on the North Fork of the Sun River about 24 miles northwest of Augusta, Montana. The dam was designed by the Bureau of Reclamation (Reclamation) and constructed by the Utah Construction Company in 1929. The dam is

operated and maintained by the Greenfields Irrigation District with oversight by Reclamation's Montana Area Office (MTAO) in Billings, Montana. The Irrigation District normally operates the dam to maximize reservoir storage for distribution of water during the irrigation season. The reservoir has a storage capacity of about 96,477 acre-feet at the top of the active conservation pool, elevation 4724.0.

Gibson Dam is a massive concrete arch structure with a structural height of 199 feet and a hydraulic height of 195 feet. The crest of the dam is 15 feet wide and approximately 960 feet long at elevation 4725.5. Parapet walls are located on both the upstream and downstream edges of the crest, with the top of the parapets at elevation 4729.0. For additional details, see the dam drawings in Appendix A.

The spillway is located through the left abutment and has a funnel-shaped (or morning glory type) drop inlet just upstream from the north end of the dam. The original free-flow inlet crest was modified in 1938, and six 34-foot-wide by 12-foot-high radial gates were installed at the inlet crest. The spillway inlet crest is at elevation 4712.0. The gate operating deck is at elevation 4738.5. From the drop inlet, flows pass through a vertical transition to a 29.5-foot-diameter concrete-lined tunnel approximately 378 feet long and then discharge into an excavated channel about 150 feet long leading back to the Sun River. For additional details, see the spillway drawings in Appendix A.

The Standing Operating Procedures (SOP) [5] for Gibson Dam lists a couple of values of maximum discharge capacity for the spillway as 31,200 ft³/s at reservoir water surface (RWS) elevation 4724.0, and 41,400 ft³/s at RWS elevation 4729.0. These values are in agreement with the current discharge curve shown on drawing 28-D-791. Model studies performed in 1936 and described in Hydraulic Report 159 [6] indicate that discharges exceeding 45,000 ft³/s result in surging flows through the spillway outlet tunnel that could cause damage to the structure. Therefore, operation of the spillway in excess of 45,000 ft³/s is not recommended except under extreme emergency conditions.

The outlet works is located near the center of the arch dam. It consists of a trashrack structure, two 72-inch-diameter semi steel-lined conduits through the base of the dam, two 5-foot-square high pressure emergency slide gates, and two 60-inch regulating jet-flow gates in a concrete gate house at the downstream toe of the dam. The jet-flow gates were installed in 1972 to replace the two needle valves installed during original construction. The capacity of the outlet works is about 3,075 ft³/s at RWS elevation 4724.0.

Two 6-foot-diameter power penstocks, located to the right of the outlet works, were stubbed through the dam at elevation 4650.0 during original construction for a future power plant that has never been added. The penstocks are presently inoperative and have been sealed with timber bulkheads on the upstream face of the dam.

On June 8-9, 1964, the dam was overtopped during a rain-on-snow flood event for about 20 hours to a maximum depth of 3.23 feet above the top of the parapet wall [7] (or 6.73 feet above the dam crest). At the time of overtopping, two of the spillway gates were

completely closed, one was open 9 feet, one was open 11 feet, and two were completely open at 12 feet. It was estimated that the maximum discharge over the parapet wall was about 18,500 ft³/s, and the maximum outflow from the dam was about 56,400 ft³/s. It was also estimated that the dam would have been overtopped even if all the spillway gates had been fully opened as early as June 1. Although some minor erosion damage occurred on the left and right abutments just downstream from the dam, no significant damage occurred to the dam, its appurtenances, or to either abutment. The condition of the right abutment rock is shown in figure 1. This flood clearly pointed out the inadequate capacity of the spillway and outlet works to prevent overtopping.

Modifications to Gibson Dam were completed in 1982 to permit safe overtopping of the dam of up to 12 feet over the parapet walls. These modifications included excavation of unstable rock on both abutments just downstream from the dam, installation of groutable rock bolts to reinforce and stabilize jointed rock in the abutments, and placement of concrete caps on both abutments to help protect them during overtopping. The concrete cap is very extensive over the right abutment as shown in figure 2. The cap on the right abutment was designed with a minimum thickness of 2.5 ft but has no waterstops between slabs and no drainage provided. The design aspects of the cap are undocumented, ie. no information regarding the selection of the rock bolt pattern, length of bolts, slab thickness or extent. In addition, there are no waterstops between slabs and no drainage of the concrete overlay. The left abutment protection is less extensive with two prominent joints filled with concrete and rock bolting over the remaining abutment area. In addition, to help protect the top of the dam and the downstream face, eight splitter piers were constructed at even intervals along the top of the dam to divide the flow of water over the crest and allow aeration beneath the nappe.

III. Site Geology

Gibson Dam is located in the Sawtooth Range in northwestern Montana on the easterly flowing North Fork of the Sun River. The area is characterized by a series of steep ridges of Paleozoic sedimentary strata separated by sedimentary Mesozoic beds. The ridges were formed by thrust faults which trend north and dip from 40 to 70° to the west. The thrust faults are considered inactive.

The river has cut a mature valley across the tilted rocks, and the tributary streams have opened relatively wide valleys in the weaker shale zones between the sharp ridges of limestone. These ridges were first cut through by an east-moving glacier, and later by streams, forming what is called water gaps. Gibson Dam is built on one of the water gaps where the rock formation is all crystalline limestone and dolomite. The foundation is a crystalline limestone in regular beds which strike normal to the river and dip upstream. The valley has been smoothed and the valley bottom widened as a result of an eastward-moving glacier. The dam is founded on the lower member of the Castle Reef Dolomite [8]. The foundation varies from beds a few inches thick to massive beds eight to ten feet thick. Orientation of the beds is extremely regular, striking 5 to 8° west of north and dipping to the west at angles ranging from 70 to 86°. The bedding dips upstream and is favorably oriented with respect to the arch of the dam.



Figure 1. - Gibson Dam downstream right abutment before construction of the concrete cap.

The rock is broken by several fissures (more erodible shaly beds) which follow the bedding planes. Between these are cross fissures or large joints. In addition, there are a large number of bedding joints or numerous cross joints that break the beds into small blocks. This condition is most evident in the right abutment (figure 1).

On the right abutment, solid rock was excavated from 5 to 30 ft deep before the joints were sufficiently tight to serve as a foundation for the dam. The major joint system on the right abutment strikes about N10°E and dips about 16°SE, whereas on the left abutment it strikes about N62°E and dips moderately to steeply SE. There is a

continuous low angle joint on the right abutment which crosses the foundation excavation and corresponds to the major joint system. On the right abutment, the original contour of the rock was nearly radial, which required little shaping. The rock in the left abutment was more massive and of better quality but required more shaping for the fit of the arch. A board of consultants recommended using a gravity tangent or thrust block on the upper right abutment to tie into the foundation at a more favorable orientation, since the ground contours nearly parallel the arch tangent in this location; however, this was not done. A toe trench was excavated upstream from the axis of the dam. Grouting was performed and a complex system of piping and manifolds, with right angle bends, connects the foundation drains to horizontal pipes extending to the downstream face of the dam. The nature of the piping makes it virtually impossible to maintain and clean the drains. The grouting and drainage curtain depths do not extend as deep as would be required by current practice.

Landslide potential around the reservoir rim is considered low.

The site geology was used in determination of the erodibility of the abutments during the overtopping event in a later section.

IV. Site History

Gibson Dam was completed in 1929. The dam spillway was modified in 1939 to add the radial gates to the spillway. On June 8-9, 1964, the dam was overtopped during a rain-on-snow flood event for about 20 hours to a maximum depth of 3.23 feet above the top of the parapet wall and an estimated flow of 18,000 ft³/s. Although some minor erosion damage occurred on the left and right abutments just downstream from the dam, no significant damage occurred to the dam, its appurtenances, or to either abutment. However, this flood clearly pointed out the inadequate capacity of the spillway and outlet works to prevent overtopping. In 1981, overtopping protection was constructed over portions of both abutments. The right abutment protection consisted of extensive concrete placement with grouted rock bolting. A couple of joints were grouted in the more competent rock located on the left abutment. This work was documented in an October 1980 memorandum and under Specifications No. DC-7393 [9]. The work included installation of rock bolts and concrete caps to protect the abutments and rock downstream from erosion during flood-related overtopping (figure 2). It was concluded that the rock on the left abutment was not erodible except for two weaker beds which were reinforced with 2.5 ft of concrete and pairs of anchor bars on each side of the beds, embedded 10 ft into rock on 5 ft centers. Fully grouted rock bolts were also installed on the downstream left abutment to tie the rock together. A 2.5-ft-thick concrete cap was installed over an extensive area of the right abutment due to the fractured nature of the surface. The concrete cap was reinforced with wire mesh and anchored with fully grouted rock bolts to resist potential hydrodynamic pressures. The design did not call for waterstops in the construction joints. Weep holes were installed through the concrete on the left abutment, but drainage was not provided beneath the concrete cap on the right abutment. It has been reported that water spurts 10 to 15 ft in the air from a drill hole near a rock bolt on the right abutment when the reservoir is full. A travel report from

1980 documents the right abutment excavation performed for the foundation of the concrete cap on the right abutment [10].

Eight splitter piers were also installed on the top of the dam, spaced about 100 ft apart radially along the length, to provide aeration of the overtopping flows.

The latest Comprehensive Facility Review (CFR) examination including an inspection, evaluation of design, analysis, and construction, analysis of risk, and performance parameter technical memorandum, was completed in November 2004 [11]. An Issue Evaluation Report of Findings was completed in May 2004 discussing the results of additional static and dynamic loading at Gibson Dam [1].

Recommendation 2004-SOD-A regarding determination of the hydraulic loading on Gibson Dam abutments will be documented in this report.

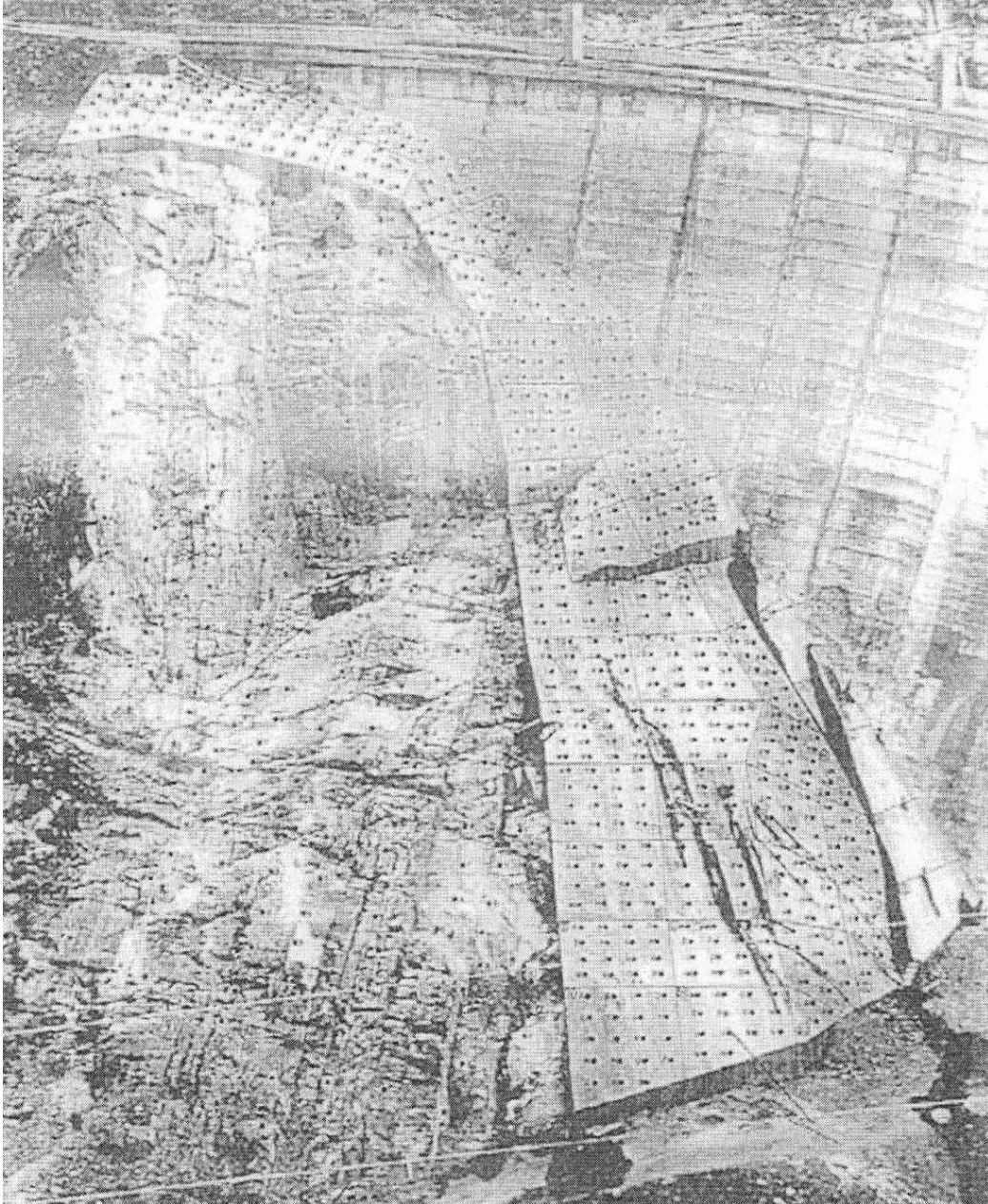


Figure 2. - Gibson Dam downstream right abutment after installation of the concrete cap and rock bolts.

V. Hydrologic Issues

The current hydrologic hazard study for Gibson Dam was completed in September 2005 [3] due to dam safety concerns related to overtopping of the dam. (More specifically, the concerns involved questions about the stability of the right abutment when subjected to flows that overtop the dam.) This study updated the 1999 Flood Frequency Analysis with peak discharges and flood volume estimates to an annual exceedance probability of 1×10^{-6} , and generated flood hydrographs to an annual exceedance probability of 1×10^{-6} . Sources of information included regional flood data from 378 United States Geological Survey (USGS) gaging stations in the regional vicinity of Gibson Dam, local flood data generated from the USGS National Flood Frequency method for determining flows up to the 100-year event, and preliminary paleoflood data developed from a site along the Sun River about 1.5 miles downstream from Gibson Dam and just downstream from the mouth of French Gulch. Table 2 shows a summary of the frequency floods developed. The hydrologic events listed in table 2 are all general storm rain-on-snow events. Local thunderstorm frequency hydrographs were not developed because the general storm hydrographs were much larger in volume and were considered to be the upper end of the hydrologic hazard.

Table 1. - General storm rain-on-snow frequency floods for Gibson Dam.

Flood Return Period (yr)	Peak Discharge (ft³/s)	7-Day Volume (ac-ft)
100	22,678	36,440
500	38,946	69,818
1000	48,186	89,723
10,000	90,900	184,957
50,000	132,212	277,130
100,000	153,394	327,962
1,000,000	243,545 *	567,427 *

* Magnitude is equivalent to the 2005 General Storm Rain-on-Snow PMF.

VI. Flood Routings

Flood routings were performed using Reclamation's computer program, FLROUT[12], and are documented in Technical Memorandum (TM) GIB-8130-CAS-2005-1 [4]. In addition, the TM documented the results of various studies and determined data such as maximum RWS elevations, freeboard values, overtopping depths, durations, and peak outflows for the 2005 general storm rain-on-snow flood frequency hydrographs.

Local thunderstorm frequency hydrographs were not provided in the September 2005 hydrologic hazard study [3] for flood routing. However, the local thunderstorm Probable Maximum Flood (PMF) hydrograph obtained from the July 2005 PMF study [13] was routed for information and comparison purposes. Maximum water surface results for the frequency flood routings and routing scenarios were plotted on a single chart to help

estimate the return period of the threshold flood (flood that brings the RWS to the top of the parapet wall on the crest of the dam) for each scenario.

The general storm rain-on-snow frequency flood hydrographs defined in the September 2005 Hydrologic Hazard report for Gibson Dam [3] have been routed through the reservoir. In order to bracket the range of possibilities for operation of the six spillway radial gates, routings were performed with all six spillway gates fully open for the duration of the flood, and with all six gates fully closed for the duration of the flood. The outlet works was assumed to be fully open and operating at capacity for all routings. This includes both jet-flow regulating gates for the outlet works. Two initial RWS elevations were considered for these routings. These included elevations 4712.0 and 4688.4. Gibson Reservoir is to be maintained at or below RWS elevation 4712.0 during the runoff season. Elevation 4712.0 is also the spillway crest elevation. Elevation 4688.4 corresponds to the end-of-April target storage of 55,000 acre-feet when above normal inflow is forecast.

Routing results indicate that overtopping of the parapet walls will begin with floods that have relatively frequent return periods. These return periods range from about 240 years to about 4600 years, depending on the initial RWS elevation at the start of the flood and whether the spillway gates are all open or all closed. See figure 3 for more details. Whatever the scenario, the inadequacy of the spillway and outlet works to prevent dam overtopping for floods with return periods greater than 4600 years is clearly indicated.

Various maximum values of overtopping for the various frequency floods routed with different combinations of initial RWS elevation and spillway gate operation are shown in table 3 and figure 3. The maximum overtopping for the 1,000,000-year flood event is practically the same whether the spillway gates are fully open or fully closed for the duration of the flood. Maximum overtopping is 14.7 feet when the gates are fully open and 14.9 feet when the gates are fully closed. This is due to the relatively small capacity of the spillway and small storage capacity of the reservoir as compared to the large discharge and volume of the 1,000,000-year flood. (The magnitude of the 1,000,000-year flood hydrograph is equivalent to the 2005 general storm rain-on-snow PMF hydrograph, both in peak discharge and volume.) These depths of overtopping are almost 3 feet higher than the design overtopping depth (12 feet) used for the overtopping protection modifications completed in 1982.

The overtopping discharges from table 3 for the 100,000-year event are in the same ballpark as the design overtopping discharge (99,800 ft³/s) used for the modifications completed in 1982. However, the overtopping discharges for the 1,000,000-year event are 80 to 83 percent greater than the design overtopping discharge.

Table 2. - Summary of frequency flood routing results for Gibson Dam.

Initial RWS Elevation = 4712.0
Six of Six Spillway Gates Fully Closed
Outlet Works Fully Open

Flood Return Period (yrs)	Maximum RWS Elevation (ft)	Freeboard on Parapet Wall ^A (ft)	Maximum Total Discharge (ft³/s)	Maximum Outlet Works Discharge (ft³/s)	Maximum Spillway Discharge (ft³/s)	Maximum Discharge over Parapet Wall (ft³/s)
100	4726.55	2.5	5882	3099	2783	0
500	4731.14	-2.1	25,091	3142	12,852	9098 ^B
1000	4732.36	-3.4	39,039	3153	16,283	19,603 ^C
10,000	4735.91	-6.9	88,733	3185	27,671	57,877 ^D
50,000	4738.29	-9.3	129,862	3207	36,380	90,276 ^E
100,000	4739.44	-10.4	150,949	3217	40,296	107,436 ^F
1,000,000	4743.86	-14.9	240,519	3256	54,683	182,580 ^G

^A Negative values indicate magnitude of overtopping the parapet wall.

^B Parapet wall is overtopped for up to 20 hours.

^C Parapet wall is overtopped for up to 26 hours.

^D Parapet wall is overtopped for up to 45 hours.

^E Parapet wall is overtopped for up to 57 hours.

^F Parapet wall is overtopped for up to 61 hours.

^G Parapet wall is overtopped for up to 78 hours.

The maximum duration of overtopping for the 1,000,000-year flood ranges from approximately 43 hours when all six spillway gates are fully open, to approximately 78 hours when all six spillway gates are fully closed. These durations are considered long enough to present a significant hydrodynamic loading on the downstream abutments due to impinging flows on the abutment surfaces.

Based on the substantial increase to the hydrodynamic loading on the abutments from the 1,000,000-year flood event, the existing overtopping protection at Gibson Dam should be reevaluated for adequacy. However, due to the remoteness of the event, this question may be better evaluated from a risk standpoint.

Even though the loading from the 100,000-year event is more similar to the design values used for the existing overtopping protection, it is recommended that a trajectory analysis be conducted to verify the location of impact of the overtopping discharge jet.

These routing results are considered appropriate for use in evaluating potential hydrologic overtopping and the resulting hydrodynamic loading on the downstream

abutments from a risk-analysis perspective. The results are also appropriate to use in making trajectory computations for the overtopping flow.

A plan view of the dam showing the outline of the morning glory spillway, dam and downstream topography is shown in Appendix A.

Routing the flood with initial reservoir elevation 4712 and the spillway gates closed leads to development of a maximum reservoir elevation, and thus, a conservative estimate of the overtopping flow. A discharge coefficient for overtopping of the dam is used that also influences the reservoir elevation. The reservoir elevation and discharge information from these routings was used in the following analysis of the flow trajectory during overtopping.

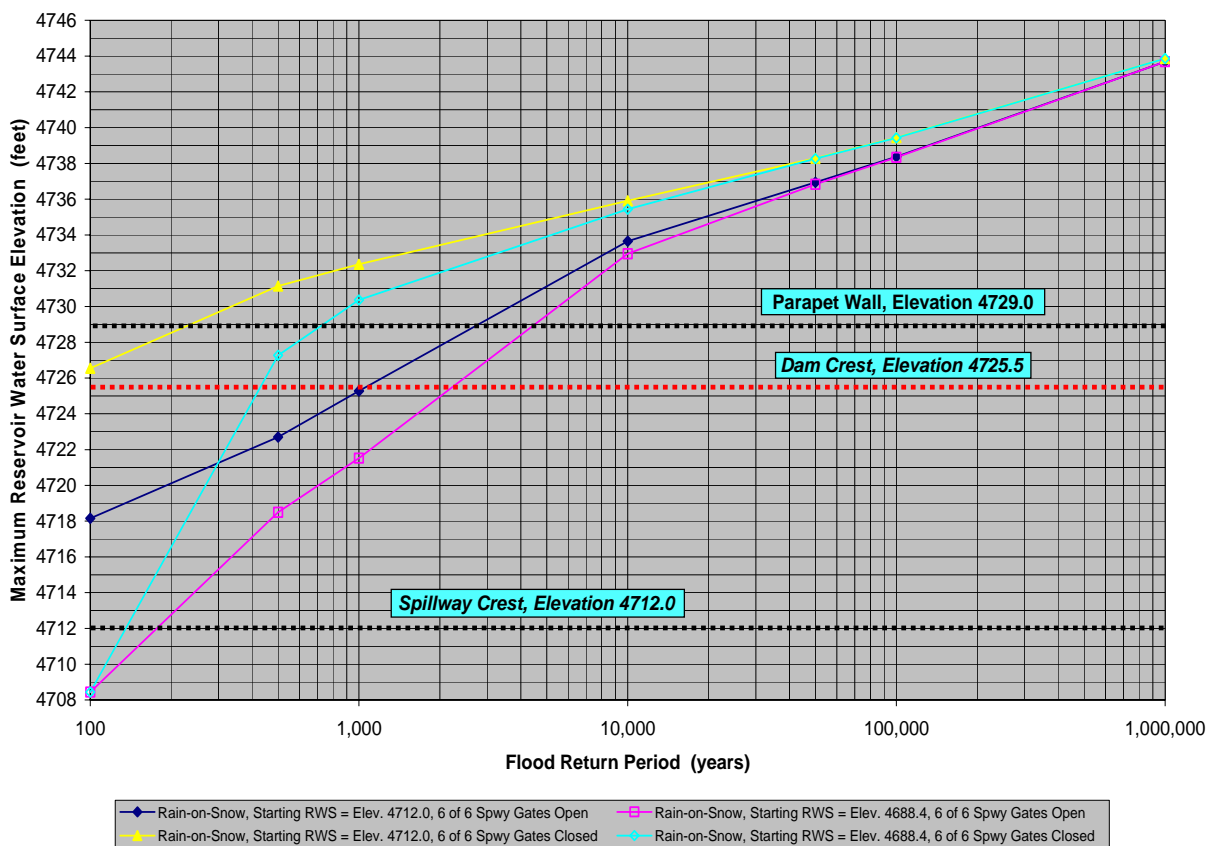


Figure 3. - Gibson Dam frequency flood routing results for the various storm events, initial reservoir elevations and spillway gate operations.

VII. Freeboard

Overtopping occurs during the PMF; therefore, there is no freeboard under that flow. Freeboard only exists for certain fairly low frequency events depending upon the initial reservoir water surface and whether or not the spillway gates are open or closed during the flood routing. The expected freeboard amounts are summarized in table 4 based upon the results shown in table 3 from [4].

Table 3. - Summary of frequency flood routing results for events with freeboard on the parapet wall.

Routing Condition	Flood Return Period (yrs)	Maximum RWS Elevation (ft)	Freeboard on Parapet Wall (ft)	Maximum Total Discharge (ft³/s)	Maximum Outlet Works Discharge (ft³/s)	Maximum Spillway Discharge (ft³/s)
RWS El.4712, gates fully closed	100	4726.55	2.5	5,882	3,099	2,783
RWS El.4688.4, gates fully closed	500	4727.27	1.7	7,120	3,106	4,014
RWS El.4712, gates fully open	1000	4725.28	3.7	37,033	3,088	33,945
RWS El.4688.4, gates fully open	1000	4721.52	7.5	25,313	3,052	22,260

It is assumed that these values are appropriate and acceptable under normal operating conditions.

VIII. Tailwater Information

Information regarding the tailwater expected at the toe of the dam was obtained for the PMF to allow determination of the flow characteristics through the tailwater and potential for reduced loading under the tailwater. Bruce Fienberg, D-8540, performed a very preliminary estimate of the PMF tailwater using a MIKE11 1D model. Overtopping but no breach of the dam was assumed. The modeling extended about 3 miles downstream, and made use of 22 cross sections. Terrain data used to create the cross sections was USGS 10-meter, level 2 DEMs. A PMF flood routing output file, which describes the discharge over the top of the dam was provided by Steve Latham (D-8110). The outflow hydrograph from the flood routing was used as an inflow boundary condition to the MIKE11 model. A cross section was set up at the dam crest location, with a geometry and crest elevation that matches the crest structure. This allowed for a simulation of the drop that takes place between the dam crest and the downstream channel at the toe of the dam. The Manning's roughness for the downstream channel was assumed to be 0.045.

Figure 4 shows the result of the MIKE11 modeling for the tailwater at the toe of Gibson dam under the PMF [14]. The maximum elevation near the toe of the dam occurred at about 38 hrs into the routing with El. 4669.9 ft.

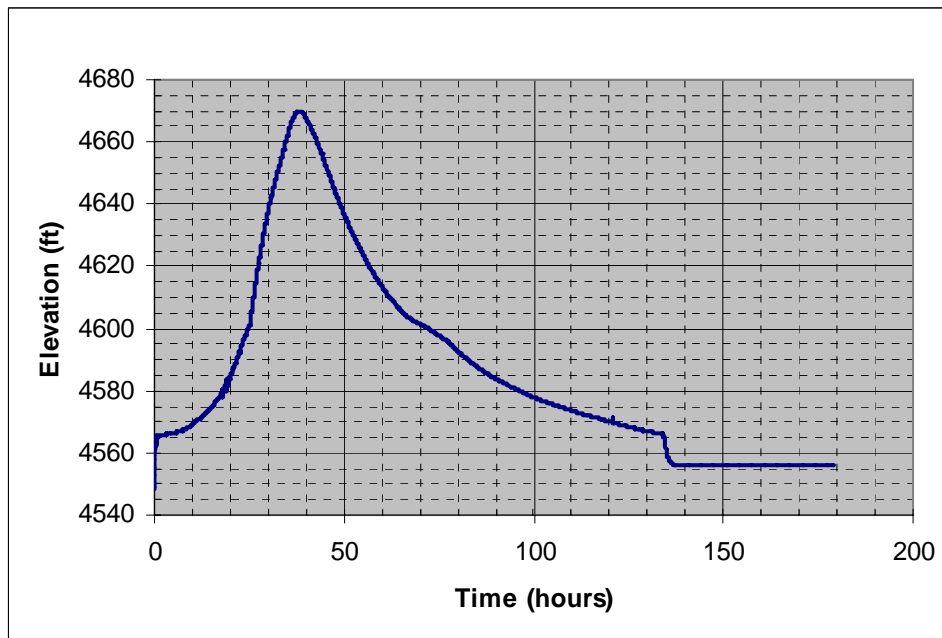


Figure 4. - Result of a preliminary tailwater study for the toe of Gibson Dam under the PMF. The maximum tailwater occurs about 38 hours into the routing with an elevation of 4669.9 ft.

IX. Hydraulic Loading

The focus of this document is to determine the hydraulic loading associated with the PMF from the November 2005 flood routing [4]. The loading is not concerned with the spillway or outlet works flows but only the amount of water going over the top of the dam parapet walls. Several aspects of the overtopping need to be addressed:

1. The jet characteristics including the jet trajectory, spread of the jet, and the location of the impingement both above and below the tailwater.
2. Computation of the load or stream power associated with the jet impingement
3. Evaluation of the effectiveness of the protective abutment treatment or rock to withstand the loading from the jet.

The following are the necessary parameters:

- $Q_{\max}=182,580 \text{ ft}^3/\text{s}$, total duration of overtopping = 78 hours
- Parapet wall El. 4729.0 ft
- Top of dam El. 4725.5 ft
- Base of dam approximately El. 4625 ft
- Width of dam crest $W=15$ ft
- Depth of overtopping above the parapet walls under the PMF = 14.9 ft
- Dam crest length $L = 960$ ft on a 405-ft radius at the upstream vertical dam face
- 8 piers on the dam to El. 4741 ft
- Tailwater in the river at the toe of the dam is about El. 4670 ft under the PMF.

Assumptions:

- Chose the worst-case scenario for the PMF or 1,000,000 year overtopping event from table 3 corresponding to initial reservoir water surface El. 4712, spillway gates fully closed, outlet works fully open
- No length deducted from the dam crest length for the 8 splitter piers
- Assume parapet walls are structurally sound and will not fail during a flood event
- Assume flow jet will spring free from the downstream parapet wall, similar to a sharp-crested weir and that the splitter walls will provide adequate aeration of the flow.

A. Definitions

The schematic on figure 5 shows the overtopping situation at Gibson Dam with definition of the important parameters of a free falling jet into a plunge pool or potentially impacting a surface above the plunge pool.

D_i = diameter of the jet at issuance from the dam

D_j = jet thickness at impact with the plunge pool or on a surface

D_{out} = outer dimension of the jet including the inner core of the jet and the jet spread

t_i = jet thickness or overtopping depth at issuance from the dam

t_j = jet thickness at impact with the plunge pool or on a surface

$H = H_{over\ top}$ = total head above the opening or over the crest

V_i = mean jet velocity at issuance from the dam

V_j = mean jet velocity at impact with the plunge pool or on a surface

Y = total plunge pool depth

Z = difference between upstream and downstream water levels

θ_i = jet angle from horizontal at issuance from the dam

δ_{out} = angle of the outer jet spread in a free falling jet

α_{out} = angle of the outer jet spread in the plunge pool

The jet characteristics must be carefully determined to adequately determine the erosion or scour potential. The flow will come directly over the top of the arch dam for the Gibson Dam PMF event and will match the definition of sketch (a) in figure 5. Therefore, the initial angle of issuance is zero and the initial jet thickness or depth of overtopping is the brink depth with the parapet wall elevation 4729 as the datum.

The brink depth and initial velocity are computed from the discharge over the dam. The discharge was computed using the weir equation, $Q = CLH^{1.5}$, with C the discharge coefficient for the dam crest, L the length of the dam crest, and H the overtopping head [4]. The critical flow depth is then computed by the relationship, $d_c = (q^2/g)^{1/3}$, where q is the discharge per unit of crest length. The brink depth is then determined by the relationship developed between the critical and brink depth [15] and continuity. For the PMF overtopping of Gibson Dam the brink depth, $d_b = 0.7.43$ ft and the initial velocity at the brink is $V_i = 25.59$ ft/s.

The jet trajectory is computed for the fall through the air with spread of the jet occurring depending upon the initial turbulence of the jet. The characteristics of the jet are determined for the fall through the air to the impact point with the tailwater as shown in figure 5c. The geometry of the tailwater pool affects the jet spread and core diffusion after the free-falling jet enters the pool. The following sections address the procedures used to determine the jet characteristics.

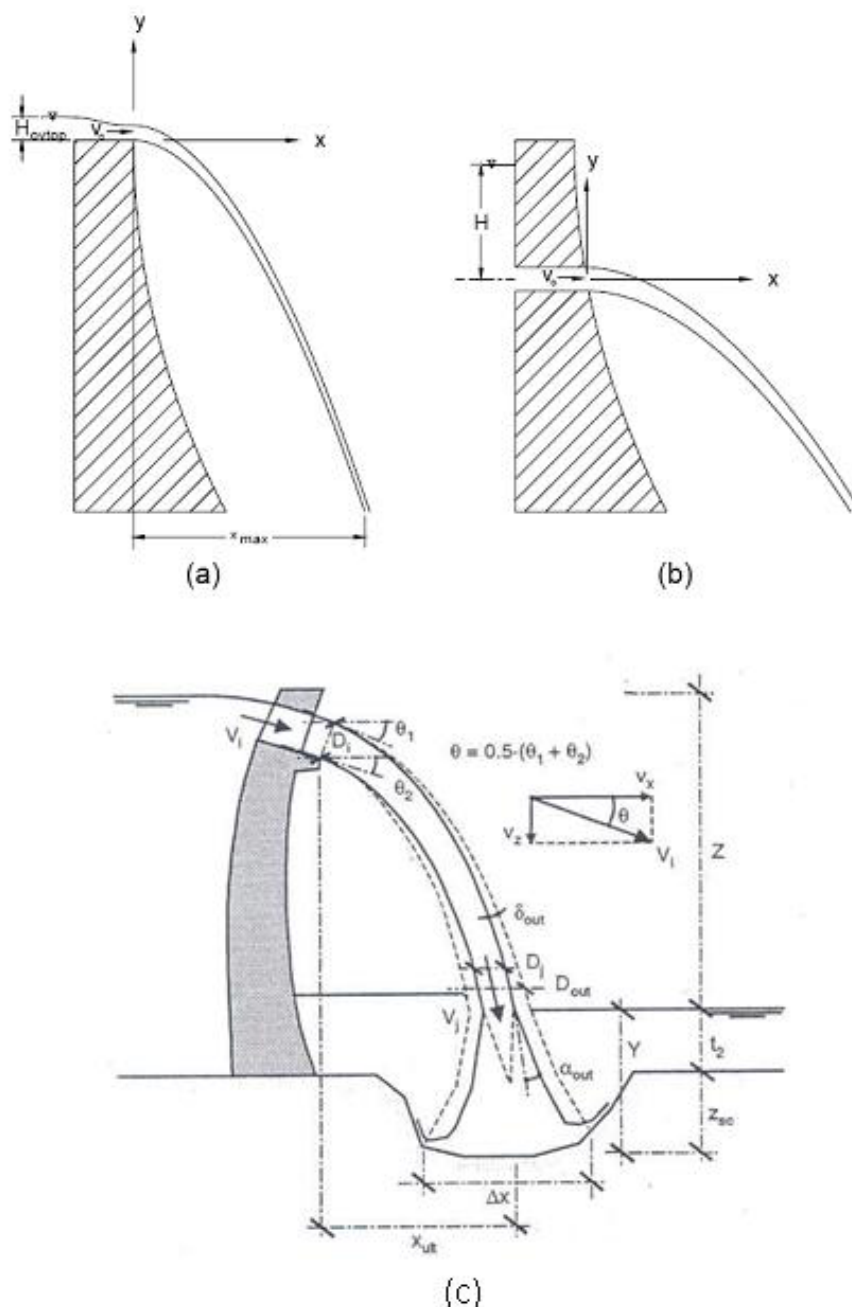


Figure 5. – Free jets (a) overtopping a dam, (b) issuing from an orifice through a dam, (c) definition sketch for parameters of a free falling jet. (Bollaert, 2002).

B. Trajectory Calculations

The flow over the top of the dam must be characterized before an evaluation of erodibility of the existing abutment treatments and/or the rock foundation may be made. The flow over the top of the dam is simply a free overfall and is computed using the equation of motion assuming no aerodynamic influences on the jet [16]. The brink depth, velocity and velocity head are used for the computation of the jet trajectory.

Using the pure form of the equation of motion produces the following equation with the downstream edge of the parapet wall as the origin of an x-y coordinate system defining the bottom edge of the jet:

$$y = x \tan \theta_i - \frac{gx^2}{2V_i^2 \cos^2 \theta_i}$$

This equation is simplified when the jet issues horizontally from the top of the dam to:

$$y = -\frac{gx^2}{2V_i^2}$$

Further manipulation of the equation may be performed by replacing the initial velocity by the velocity head, $h_v = V_i^2/2g$ producing:

$$y = -\frac{x^2}{4h_v}$$

The upper edge of the jet is defined by adding the initial depth or jet thickness to the bottom edge of the jet.

The following equation from Design of Small Dams [17] and Scour Technology [18] was derived from the equations of motion with x and y being the horizontal and vertical distances in ft from some datum depending upon whether referencing an orifice or gate, a free overtopping situation, or design of a vertical curve in a spillway chute:

$$-y = x \tan \theta_i + \frac{x^2}{4K(d + h_v)\cos^2 \theta_i}$$

This equation is similar to the pure equation of motion with the exception of the variable K, and there is an extra depth term in the denominator that is not well defined. The K factor is applied to allow conservative application of the equation depending upon the design situation. For a free falling jet, K=1 for a theoretical jet, and 0.9 for a real jet according to Small Dams [17]; and Annandale [18] and Bollaert [19] suggest 0.75.

The more puzzling aspect of the equation from Design of Small Dams is the additional depth term. When analyzing an orifice flow or a design for high velocity flow in a chute, the equation could be applied with the depth, d , and velocity head equaling the total head minus losses to that point. The equation can only be correct in an overtopping situation if the entire overtopping head were being converted to velocity head. This does not occur because until the flow springs free from the crest, a nearly hydrostatic pressure profile exists in the flow, and a portion of the energy is in the form of pressure head. This has led to some confusion in overtopping situations and a flatter trajectory resulting after adding velocity head to the total overtopping head.

In the case of Gibson Dam with free overflow over the dam, there are two factors to consider with the jet; 1.) the horizontal travel of the jet to ensure that existing concrete protection extent is adequate, and 2.) the velocity of the jet after the fall to determine impingement forces. A value of $K = 1$ is selected since the thickness of the jet substantially will prevent its break up. This produces a trajectory that is conservative with respect to the distance of the impingement from the dam. Free falling jet trajectories were also computed for K factors of 0.75, 0.9, and 1. As a reference, a K factor of 1.5 or greater is used when designing a convex vertical curve to flatten the curve and prevent the jet from lifting off the spillway chute invert [17]. Table 11 and figure 12 in Appendix B show the results of the sensitivity study on K factors for the PMF.

The trajectory for Gibson dam is shown on figure 6 with the initial jet thickness shown as the brink depth. Contraction of the inner core of the jet and the spread of the jet as it falls through the air are not shown on figure 6.

The final trajectory for the jet overtopping Gibson Dam is shown in a sectional view on figure 6. This trajectory through the air shows the simple jet trajectory from the equation of motion. No spread of the outer diameter of the jet is shown in figure 6 or with the footprint of the jet on the abutments and or impact at the tailwater on figure 7. The plot of the concrete surface shows the distance radially downstream from the dam parapet and the elevations of the surfaces. Where the trajectory intersects or goes beyond the surface is where the jet will impact on the downstream rock.

Figure 7 shows the predicted footprint of the jet as it would impinge on the rock or concrete overlay on the abutments and into the tailwater pool at El. 4670. The concern is the pressure or force transmitted by the power of the jet as it impacts the surfaces above and below the tailwater.

The zone of impingement on the abutments above the tailwater is of concern. From figure 7 the jet will impinge on the concrete protection or the abutment rock. The key is determining the power in the flow or pressure force exerted onto the surfaces by the flow impingement. The flow jet will impinge on the rock above the tailwater in the zone shown on figure 7. The jet will impinge on the rock beyond the concrete protection between El. 4710 and El 4670 or the maximum tailwater at the PMF. The jet will then impact into the tailwater.

The jet will not break up as it travels through the air because the length predicted to break up is much greater than the height of fall. The free-falling jet will, however, experience spread due to turbulence and contraction of the core due to gravity. As the jet enters the tailwater other factors combine to influence the dispersion of the core and spread of the outer edges of the jet.

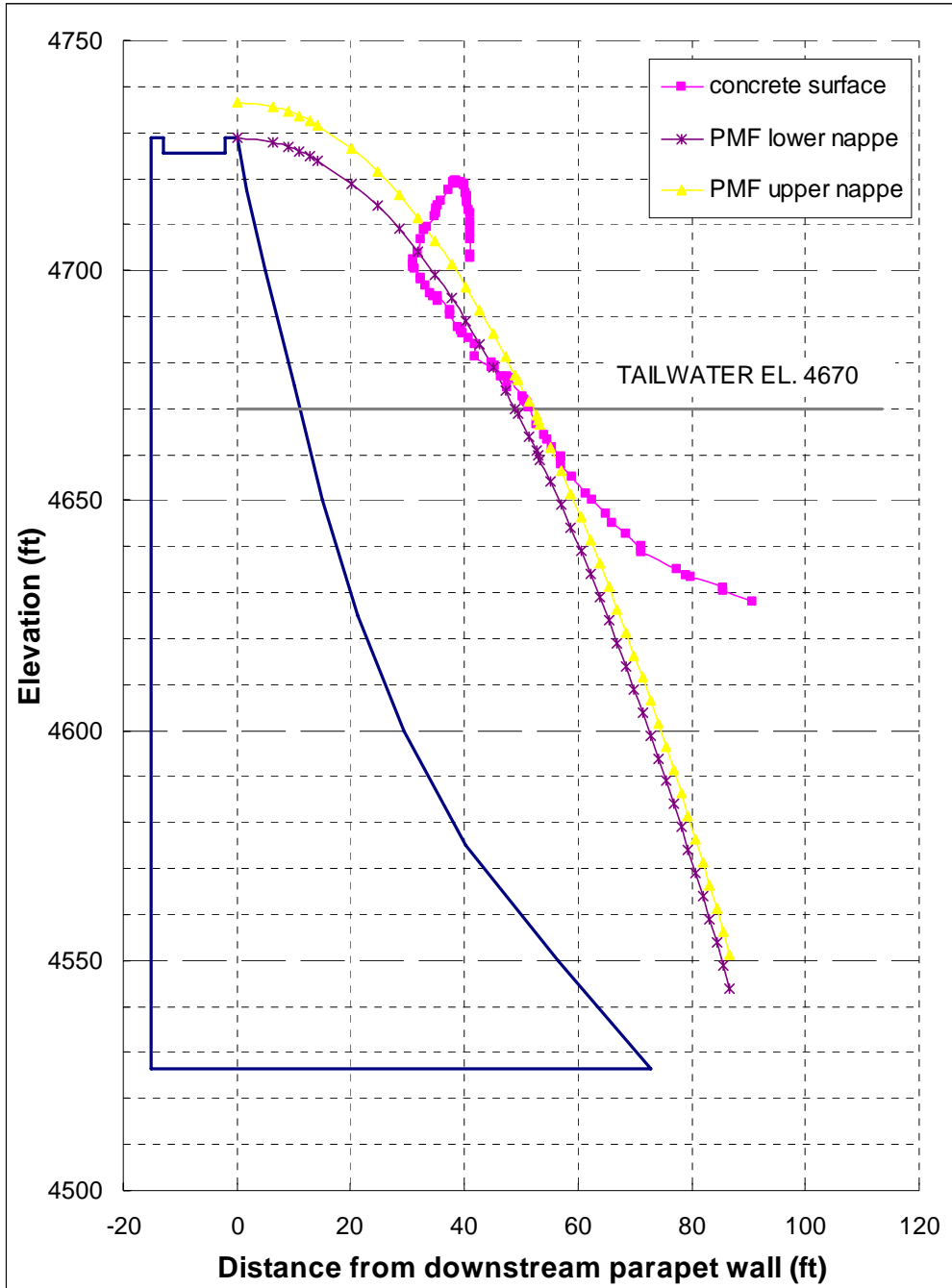


Figure 6. - Sectional view of the final trajectory profile for the PMF for Gibson Dam through dam section A-A aligned with the river channel.

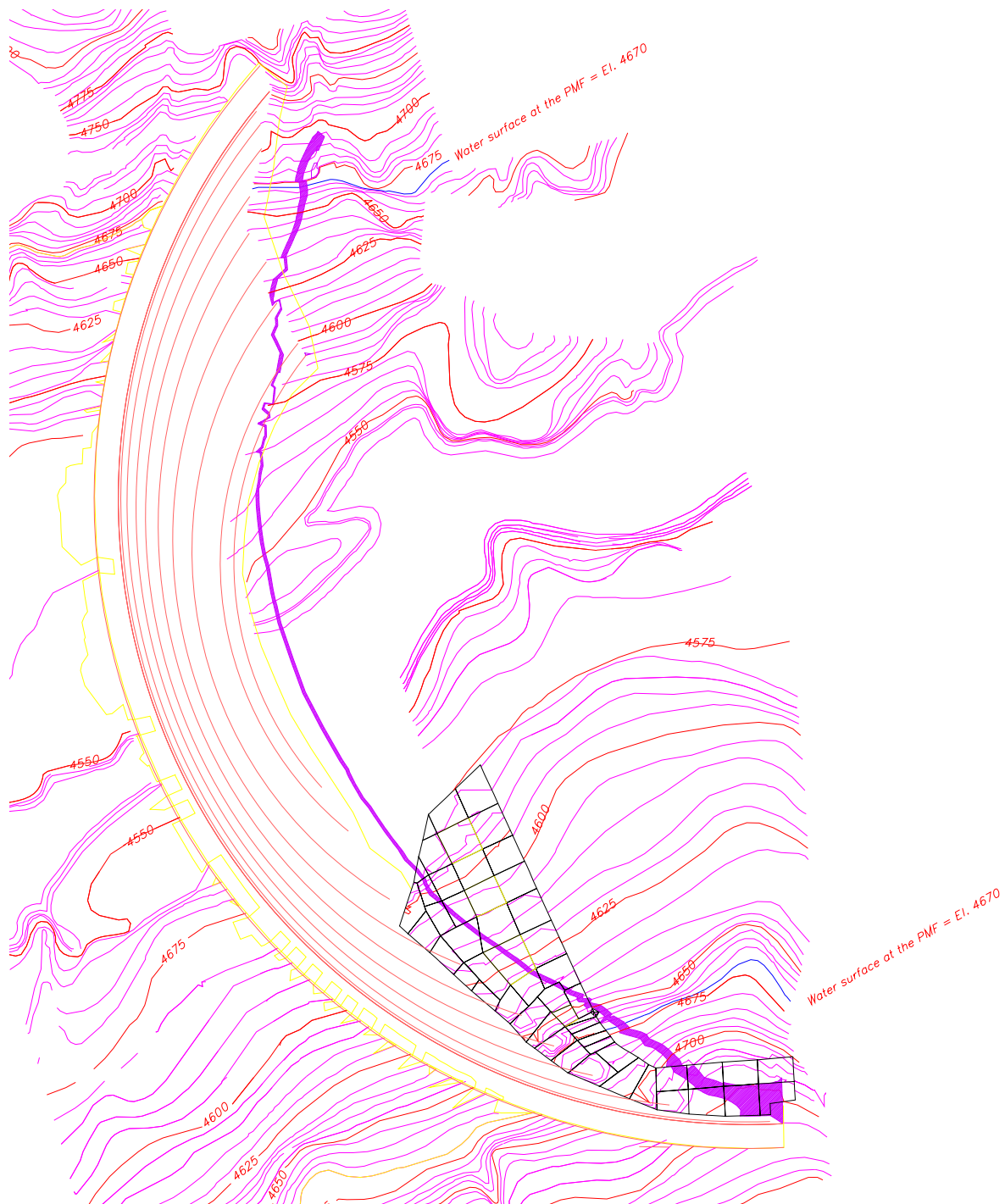


Figure 7. - Footprint of the trajectory with no spread of the jet for the PMF overtopping at Gibson Dam. Note the location of the footprint extends beyond the right abutment protection between contour elevations 4660 and 4710. The tailwater for the PMF is shown on the plan view in blue at El. 4670.

1. Jet Spread in the Free Fall

The fall height of the jet varies across the width of the dam, depending on whether it impinges on the abutments or falls to the tailwater at El. 4670 for the PMF. The fall height is computed as the difference between the reservoir El. 4743.9 and the impingement location. In the case of fall to the tailwater the fall height, Z , is equal to 73.9 ft and is the maximum fall because the jet will impinge on the abutments sooner. The following equations predict the dimension of the inner jet core and outer jet spread using empirical data from experiments based upon circular jets. For many applications, such as jets issuing from gates, the initial depth may be converted to an equivalent circular diameter and that parameter used for the initial depth, D_i . For overtopping, the footprint of the jet is expected to remain rectangular and no conversion to a circular or round jet is made. There is no extensive data for rectangular jets; therefore, the equations for round jets were applied for the analysis for Gibson Dam with the rectangular jet thickness.

The contraction of the core of a round jet at the point of impingement or impact, D_j , due to gravity is computed for round jets by using equation 5.46 from Annandale [18]:

$$D_j = D_i \sqrt{\frac{V_i}{V_j}}$$

where the D_i and V_i are the initial depth of overtopping and the initial velocity of the jet and V_j is the velocity at the location of impact. This equation is easily used to convert to a rectangular jet by using continuity to produce a jet thickness, t_j , at the point of impact given by:

$$t_j = t_i \left(\frac{V_i}{V_j} \right)$$

where the t_i and V_i are the initial brink depth and the initial velocity of the jet and V_j is the velocity at the location of impact. The velocity at the point of impact is given by equation 5.47 from Annandale [18] with Z equal to the total drop from the reservoir:

$$V_j = \sqrt{V_i^2 + 2gZ}$$

Performing these two computations for Gibson dam at the impact with the tailwater produces a jet thickness, $t_j = 2.58$ ft and $V_j = 73.58$ ft/s. The spread of the outer portion of the jet which includes aeration of a turbulent jet is computed by two different, but similar methods. Ervine and Falvey [20] and Ervine et. al. [21] determined that the total dimension of the outer spread of the jet, D_{out} , is equal to:

$$D_{out} = D_i + 2 * 0.38(T_u L_j)$$

where T_u is the turbulence intensity of the jet based upon values from table 4 for various types of jet issuance, and L_j is the length of the jet along the trajectory as it falls through the air to the impingement location. For Gibson Dam overtopping the length of the trajectory to the tailwater is 127.8 ft and is computed by equation 5.37 from Annandale [18] integrated to horizontal distance x :

$$L_j = x \sqrt{1 + \left[\tan \theta - \frac{2x}{4Kh_v \cos^2 \theta} \right]^2}$$

The characteristics of the thick jet overtopping the dam led to selection of a turbulence intensity, $T_u = 0.03$ from table 4. Inputting these values into the above equation for the dimension of the outer jet spread produces $D_{out} = 10.35$ ft at El. 4670.

Table 4. - Table of turbulence intensities for free falling jets Bolleart (2002).

Structure type	Turbulence Intensity
free overfall	0.00-0.03
ski jump	0.03-0.05
Valve	0.03-0.08

The outer spread of the jet determined by the other method is computed by equations 5.48 and 5.49 from Annandale (18):

$$\varepsilon = \frac{1.14T_u V_i^2}{g} \cdot \left[\sqrt{\frac{2L_j}{t_i Fr_i^2} + 1} - 1 \right]$$

where Fr_i is the Froude number of the initial jet and V_i is the initial velocity of the jet then:

$$D_{out} = t_i \left(\frac{V_i}{V_j} \right) + 2\varepsilon$$

The value of D_{out} using this method is 17.1 ft at El. 4670. Comparing this result to that using the simpler equation above shows that both methods produce similar results and certainly either could be used. Table 5 shows the result of the jet characteristics determined for the free-falling jet at Gibson Dam under the PMF flow rate.

Table 5. - Free-falling jet characteristics for the PMF overtopping at Gibson Dam.

Vertical distance (y) from parapet elevation (ft)	Horizontal distance (x) from downstream parapet	Elevation of lower nappe (ft)	Elevation of upper nappe (ft)	Trajectory length (ft)	Jet angle of impingement (degrees)	Outer width of jet (ft)	Velocity of jet at impact with various elevations. (ft/s)
0.00	0.00	4729.00	4736.43	0.00	0.00	7.43	40.18
-1.00	6.38	4728.00	4735.43	6.68	23.22	7.59	40.97

Vertical distance (y) from parapet elevation (ft)	Horizontal distance (x) from downstream parapet	Elevation of lower nappe (ft)	Elevation of upper nappe (ft)	Trajectory length (ft)	Jet angle of impingement (degrees)	Outer width of jet (ft)	Velocity of jet at impact with various elevations. (ft/s)
-2.00	9.02	4727.00	4734.43	9.87	31.24	7.66	41.75
-3.00	11.05	4726.00	4733.43	12.57	36.61	7.72	42.51
-4.00	12.75	4725.00	4732.43	15.06	40.63	7.78	43.27
-5.00	14.26	4724.00	4731.43	17.42	43.81	7.83	44.00
-10.00	20.17	4719.00	4726.43	28.40	53.60	8.08	47.52
-15.00	24.70	4714.00	4721.43	38.86	58.96	8.32	50.80
-20.00	28.52	4709.00	4716.43	49.13	62.47	8.55	53.87
-25.00	31.89	4704.00	4711.43	59.30	65.00	8.78	56.78
-30.00	34.93	4699.00	4706.43	69.43	66.95	9.02	59.55
-35.00	37.73	4694.00	4701.43	79.52	68.49	9.25	62.20
-40.00	40.33	4689.00	4696.43	89.59	69.77	9.48	64.73
-45.00	42.78	4684.00	4691.43	99.65	70.84	9.70	67.17
-50.00	45.09	4679.00	4686.43	109.70	71.75	9.93	69.53
-55.00	47.29	4674.00	4681.43	119.74	72.55	10.16	71.81
-59.00	48.98	4670.00	4677.43	127.76	73.12	10.35	73.58

2. Jet Break Up Length in Free Fall

The following equations, from Ervine, et al. [20], were used to determine the length to the expected break up of the jet as it falls or travels through the air, L_b :

$$C = \frac{1}{\sqrt{\frac{2L_b}{D_i Fr_i^2} + 1} * \left(\sqrt{\frac{2L_b}{D_i Fr_i^2} + 1} - 1 \right)^2}$$

$$C = 1.14 T_u Fr_i^2$$

Again, the turbulence intensity is selected from table 4 as 0.03. The result of this computation by trial and error produces, $L_b = 140$ ft.

Additionally, the length of the jet to break up may be computed by a few other methods.

$$L_b = \frac{1.05 * t_i Fr_i^2}{C^{0.82}}$$

Using this equation, $L_b = 149$ ft, about 9 ft more than the break up length computed by the more complex trial and error method from the above equation. There are other methods to predict the distance to jet break up, but either of these previously stated methods is preferred.

The result of this computation is that no break up of the jet is expected because the maximum fall distance is 73.9 ft to the tailwater and the break up distance, predicted by either method, is much larger.

a) Jet Trajectories for Various Overtopping Flows

The previous calculation for the PMF event showed impingement beyond the existing concrete protection on the right abutment. As a result, investigation of the jet trajectories for other flood events was requested. Flood frequencies of 500, 1000, 10000, 50000, and 100000-year events from table 6 of the Flood Routing TM were used [4]. The discharges and initial reservoir elevations from table 6 of the Flood Routing TM are shown in this report at table 2. Table 6 and figure 8 shows the family of trajectories determined for the various flood frequencies, including the previous result for the PMF.

The horizontal (x) and vertical (y) distances are given from the downstream dam parapet wall. The lower nappe begins at the elevation of the parapet wall, El. 4629.5 and is computed using the horizontal and vertical displacements from the trajectory equation. The upper nappe was determined by adding the initial overtopping brink depth to the lower nappe elevation.

Figure 8 also shows the downstream edge of the right abutment concrete protection as a line. The “hook” in the line is a result of the protection being a lower elevation at the far right end of the protection, then increasing in elevation before consistently decreasing in elevation as the abutment drops down to the river channel.

The simplified presentation of the trajectories with the downstream outline of the right abutment concrete protection allows a quick general determination of whether or not the trajectory for a specific frequency event will impinge onto the protection. The trajectories that travel beyond the line for the protection will impinge downstream and those that are between the dam and the line will fall onto the protection. It appears that the flood frequency events up to the 100,000 year event will all fall on the existing right abutment protection, whereas those with frequency exceeding 100,000 years will travel beyond the protection and impinge on the rock abutment. The upper nappe of the 100,000 year event is close to travelling beyond the protection near the top of the protection and might need slightly more careful investigation if it is determined that enough energy exists in the flow to be of concern at this high elevation.

A risk analysis could be performed with this information to determine if the protection is adequate.

select y	PMF			500			1000			10000			50000			100000		
	x	el. Lower	el. Upper	x	el. Lower	el. Upper	x	el. Lower	el. Upper	x	el. Lower	el. Upper	x	el. Lower	el. Upper	x	el. Lower	el. Upper
0	0.00	4729.00	4736.43	0.00	4729.00	4730.01	0.00	4729.00	4730.68	0.00	4729.00	4732.45	0.00	4729.00	4733.65	0.00	4729.00	4734.22
-2	9.02	4727.00	4734.43	3.32	4727.00	4728.01	4.29	4727.00	4728.68	6.15	4727.00	4730.45	7.13	4727.00	4731.65	7.56	4727.00	4732.22
-4	12.76	4725.00	4732.43	4.69	4725.00	4726.01	6.06	4725.00	4726.68	8.70	4725.00	4728.45	10.09	4725.00	4729.65	10.69	4725.00	4730.22
-6	15.62	4723.00	4730.43	5.75	4723.00	4724.01	7.42	4723.00	4724.68	10.65	4723.00	4726.45	12.35	4723.00	4727.65	13.09	4723.00	4728.22
-8	18.04	4721.00	4728.43	6.64	4721.00	4722.01	8.57	4721.00	4722.68	12.30	4721.00	4724.45	14.27	4721.00	4725.65	15.12	4721.00	4726.22
-10	20.17	4719.00	4726.43	7.42	4719.00	4720.01	9.59	4719.00	4720.68	13.75	4719.00	4722.45	15.95	4719.00	4723.65	16.90	4719.00	4724.22
-12	22.10	4717.00	4724.43	8.13	4717.00	4718.01	10.50	4717.00	4718.68	15.07	4717.00	4720.45	17.47	4717.00	4721.65	18.52	4717.00	4722.22
-14	23.87	4715.00	4722.43	8.78	4715.00	4716.01	11.34	4715.00	4716.68	16.27	4715.00	4718.45	18.87	4715.00	4719.65	20.00	4715.00	4720.22
-16	25.51	4713.00	4720.43	9.39	4713.00	4714.01	12.12	4713.00	4714.68	17.40	4713.00	4716.45	20.17	4713.00	4717.65	21.38	4713.00	4718.22
-18	27.06	4711.00	4718.43	9.96	4711.00	4712.01	12.86	4711.00	4712.68	18.45	4711.00	4714.45	21.40	4711.00	4715.65	22.68	4711.00	4716.22
-20	28.53	4709.00	4716.43	10.50	4709.00	4710.01	13.56	4709.00	4710.68	19.45	4709.00	4712.45	22.56	4709.00	4713.65	23.90	4709.00	4714.22
-22	29.92	4707.00	4714.43	11.01	4707.00	4708.01	14.22	4707.00	4708.68	20.40	4707.00	4710.45	23.66	4707.00	4711.65	25.07	4707.00	4712.22
-24	31.25	4705.00	4712.43	11.50	4705.00	4706.01	14.85	4705.00	4706.68	21.31	4705.00	4708.45	24.71	4705.00	4709.65	26.18	4705.00	4710.22
-26	32.52	4703.00	4710.43	11.97	4703.00	4704.01	15.46	4703.00	4704.68	22.18	4703.00	4706.45	25.72	4703.00	4707.65	27.25	4703.00	4710.22
-28	33.75	4701.00	4708.43	12.42	4701.00	4702.01	16.04	4701.00	4702.68	23.01	4701.00	4704.45	26.69	4701.00	4705.65	28.28	4701.00	4706.22
-30	34.94	4699.00	4706.43	12.85	4699.00	4700.01	16.60	4699.00	4700.68	23.82	4699.00	4702.45	27.63	4699.00	4703.65	29.28	4699.00	4704.22
-32	36.08	4697.00	4704.43	13.28	4697.00	4698.01	17.15	4697.00	4698.68	24.60	4697.00	4700.45	28.53	4697.00	4701.65	30.24	4697.00	4702.22
-34	37.19	4695.00	4702.43	13.68	4695.00	4696.01	17.68	4695.00	4696.68	25.36	4695.00	4698.45	29.41	4695.00	4699.65	31.17	4695.00	4702.22
-36	38.27	4693.00	4700.43	14.08	4693.00	4694.01	18.19	4693.00	4694.68	26.09	4693.00	4696.45	30.26	4693.00	4697.65	32.07	4693.00	4698.22
-38	39.32	4691.00	4698.43	14.47	4691.00	4692.01	18.69	4691.00	4692.68	26.81	4691.00	4694.45	31.09	4691.00	4698.65	32.95	4691.00	4698.22
-40	40.34	4689.00	4696.43	14.84	4689.00	4690.01	19.17	4689.00	4690.68	27.50	4689.00	4692.45	31.90	4689.00	4693.65	33.80	4689.00	4694.22
-42	41.34	4687.00	4694.43	15.21	4687.00	4688.01	19.64	4687.00	4688.68	28.18	4687.00	4690.45	32.69	4687.00	4691.65	34.64	4687.00	4692.22
-44	42.31	4685.00	4692.43	15.57	4685.00	4686.01	20.11	4685.00	4686.68	28.85	4685.00	4688.45	33.46	4685.00	4689.65	35.45	4685.00	4690.22
-46	43.26	4683.00	4690.43	15.92	4683.00	4684.01	20.56	4683.00	4684.68	29.50	4683.00	4686.45	34.21	4683.00	4687.65	36.25	4683.00	4688.22
-48	44.19	4681.00	4688.43	16.26	4681.00	4682.01	21.00	4681.00	4682.68	30.13	4681.00	4684.45	34.94	4681.00	4688.65	37.03	4681.00	4688.22
-50	45.10	4679.00	4686.43	16.59	4679.00	4680.01	21.43	4679.00	4680.68	30.75	4679.00	4682.45	35.66	4679.00	4683.65	37.79	4679.00	4684.22
-52	46.00	4677.00	4684.43	16.92	4677.00	4678.01	21.86	4677.00	4678.68	31.36	4677.00	4680.45	36.37	4677.00	4681.65	38.54	4677.00	4682.22
-54	46.87	4675.00	4682.43	17.25	4675.00	4676.01	22.27	4675.00	4676.68	31.96	4675.00	4678.45	37.06	4675.00	4678.65	39.28	4675.00	4680.22
-56	47.73	4673.00	4680.43	17.56	4673.00	4674.01	22.68	4673.00	4674.68	32.54	4673.00	4676.45	37.74	4673.00	4677.65	40.00	4673.00	4678.22
-58	48.58	4671.00	4678.43	17.87	4671.00	4672.01	23.09	4671.00	4672.68	33.12	4671.00	4674.45	38.41	4671.00	4675.65	40.71	4671.00	4676.22
-60	49.41	4669.00	4676.43	18.18	4669.00	4670.01	23.48	4669.00	4670.68	33.69	4669.00	4672.45	39.07	4669.00	4673.65	41.40	4669.00	4674.22
-62	50.23	4667.00	4674.43	18.48	4667.00	4668.01	23.87	4667.00	4668.68	34.24	4667.00	4670.45	39.71	4667.00	4671.65	42.09	4667.00	4672.22
-64	51.03	4665.00	4672.43	18.77	4665.00	4666.01	24.25	4665.00	4666.68	34.79	4665.00	4668.45	40.35	4665.00	4669.65	42.76	4665.00	4670.22
-66	51.82	4663.00	4670.43	19.07	4663.00	4664.01	24.63	4663.00	4664.68	35.33	4663.00	4666.45	40.98	4663.00	4667.65	43.42	4663.00	4668.22
-68	52.60	4661.00	4668.43	19.35	4661.00	4662.01	25.00	4661.00	4662.68	35.86	4661.00	4664.45	41.59	4661.00	4666.65	44.08	4661.00	4666.22
-70	53.37	4659.00	4666.43	19.63	4659.00	4660.01	25.36	4659.00	4660.68	36.39	4659.00	4662.45	42.20	4659.00	4663.65	44.72	4659.00	4664.22
-72	54.12	4657.00	4664.43	19.91	4657.00	4658.01	25.72	4657.00	4658.68	36.90	4657.00	4660.45	42.80	4657.00	4661.65	45.35	4657.00	4662.22
-74	54.87	4655.00	4662.43	20.19	4655.00	4656.01	26.08	4655.00	4656.68	37.41	4655.00	4658.45	43.39	4655.00	4659.65	45.98	4655.00	4660.22
-76	55.61	4653.00	4660.43	20.46	4653.00	4654.01	26.43	4653.00	4654.68	37.91	4653.00	4656.45	43.97	4653.00	4657.65	46.60	4653.00	4658.22
-78	56.33	4651.00	4658.43	20.73	4651.00	4652.01	26.77	4651.00	4652.68	38.41	4651.00	4654.45	44.54	4651.00	4655.65	47.21	4651.00	4656.22
-80	57.05	4649.00	4656.43	20.99	4649.00	4650.01	27.11	4649.00	4650.68	38.90	4649.00	4652.45	45.11	4649.00	4653.65	47.81	4649.00	4654.22
-82	57.76	4647.00	4654.43	21.25	4647.00	4648.01	27.45	4647.00	4648.68	39.38	4647.00	4650.45	45.67	4647.00	4651.65	48.40	4647.00	4652.22
-84	58.46	4645.00	4652.43	21.51	4645.00	4646.01	27.78	4645.00	4646.68	39.86	4645.00	4648.45	46.23	4645.00	4649.65	48.99	4645.00	4650.22
-86	59.15	4643.00	4650.43	21.76	4643.00	4644.01	28.11	4643.00	4644.68	40.33	4643.00	4646.45	46.77	4643.00	4647.65	49.57	4643.00	4648.22
-88	59.84	4641.00	4648.43	22.01	4641.00	4642.01	28.44	4641.00	4642.68	40.80	4641.00	4644.45	47.31	4641.00	4645.65	50.14	4641.00	4646.22
-90	60.51	4639.00	4646.43	22.26	4639.00	4640.01	28.76	4639.00	4640.68	41.26	4639.00	4642.45	47.85	4639.00	4643.65	50.71	4639.00	4644.22
-92	61.18	4637.00	4644.43	22.51	4637.00	4638.01	29.07	4637.00	4638.68	41.71	4637.00	4640.45	48.38	4637.00	4641.65	51.27	4637.00	4642.22
-94	61.84	4635.00	4642.43	22.75	4635.00	4636.01	29.39	4635.00	4636.68	42.16	4635.00	4638.45	48.90	4635.00	4639.65	51.82	4635.00	4640.22
-96	62.50	4633.00	4640.43	22.99	4633.00	4634.01	29.70	4633.00	4634.68	42.61	4633.00	4636.45	49.42	4633.00	4637.65	52.37	4633.00	4638.22
-98	63.15	4631.00	4638.43	23.23	4631.00	4632.01	30.01	4631.00	4632.68	43.05	4631.00	4634.45	49.93	4631.00	4635.65	52.91	4631.00	4636.22
-100	63.79	4629.00	4636.43	23.47	4629.00	4630.01	30.31	4629.00	4630.68	43.49	4629.00	4632.45	50.44	4629.00	4633.65	53.45	4629.00	4634.22
-102	64.42	4627.00	4634.43	23.70	4627.00	4628.01	30.61	4627.00	4628.68	43.92	4627.00	4630.45	50.94	4627.00	4631.65	53.98	4627.00	4632.22
-104	65.05	4625.00	4632.43	23.93	4625.00	4626.01	30.91	4625.00	4626.68	44.35	4625.00	4628.45	51.44	4625.00	4629.65	54.51	4625.00	4630.22
-106	65.67	4623.00	4630.43	24.16	4623.00	4624.01	31.21	4623.00	4624.68	44.77	4623.00	4626.45	51.93	4623.00	4627.65	55.03	4623.00	4628.22
-108	66.29	4621.00	4628.43	24.39	4621.00	4622.01	31.50	4621.00	4622.68	45.20	4621.00	4624.45	52.42	4621.00	4625.65	55.55	4621.00	4626.22
-110	66.90	4619.00	4626.43	24.61	4619.00	4620.01	31.79	4619.00	4620.68	45.61	4619.00	4622.45	52.90	4619.00	4623.65	56.06	4619.00	4624.22
-112	67.51</																	

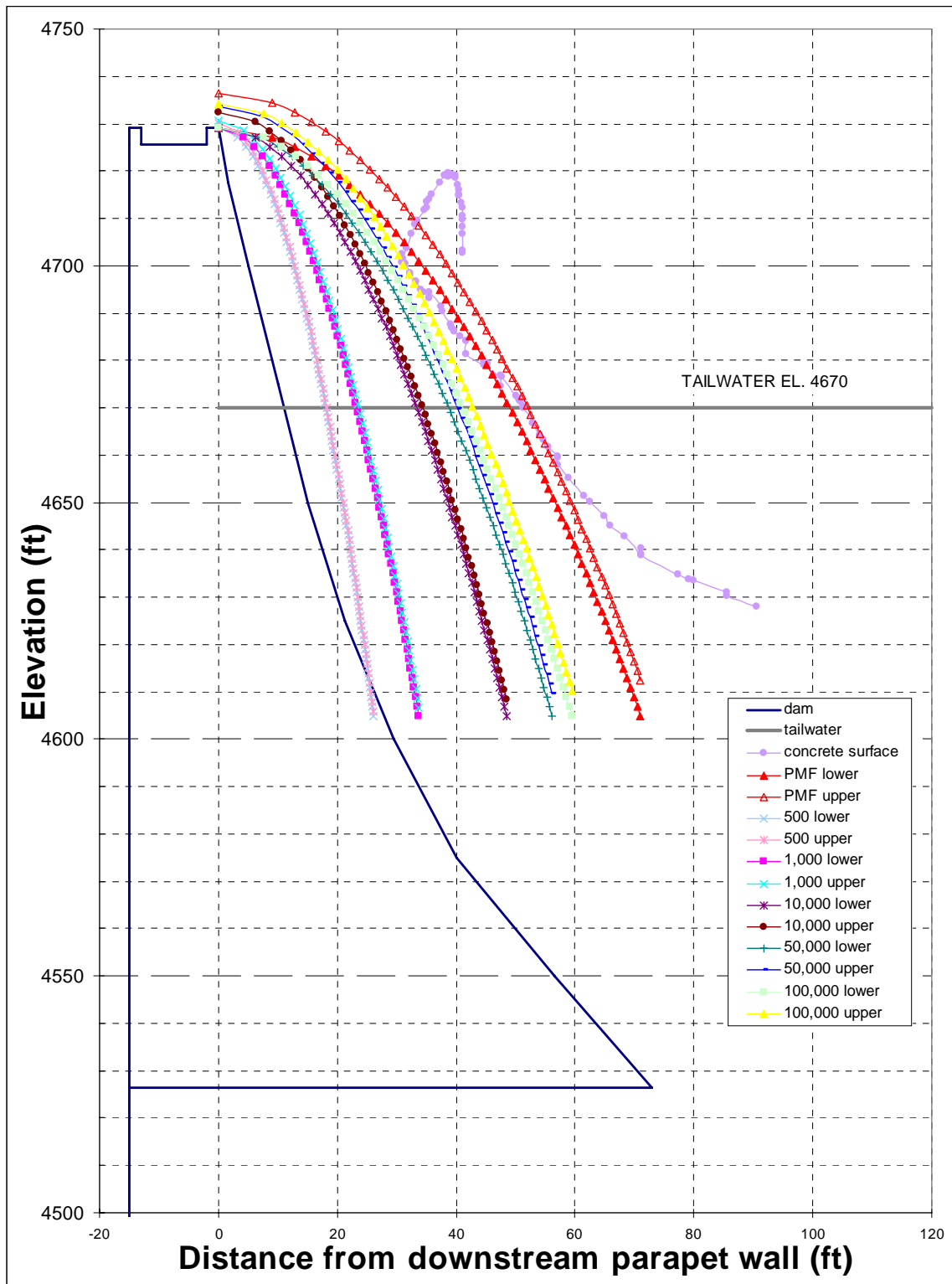


Figure 8. - Sectional view of predicted trajectories for various frequency overtopping flood events at Gibson Dam.

C. Jet Plunge Pool Characteristics

The next portion of the investigation is to determine the characteristics of the jet as it plunges into and through the plunge pool as shown on figure 9.

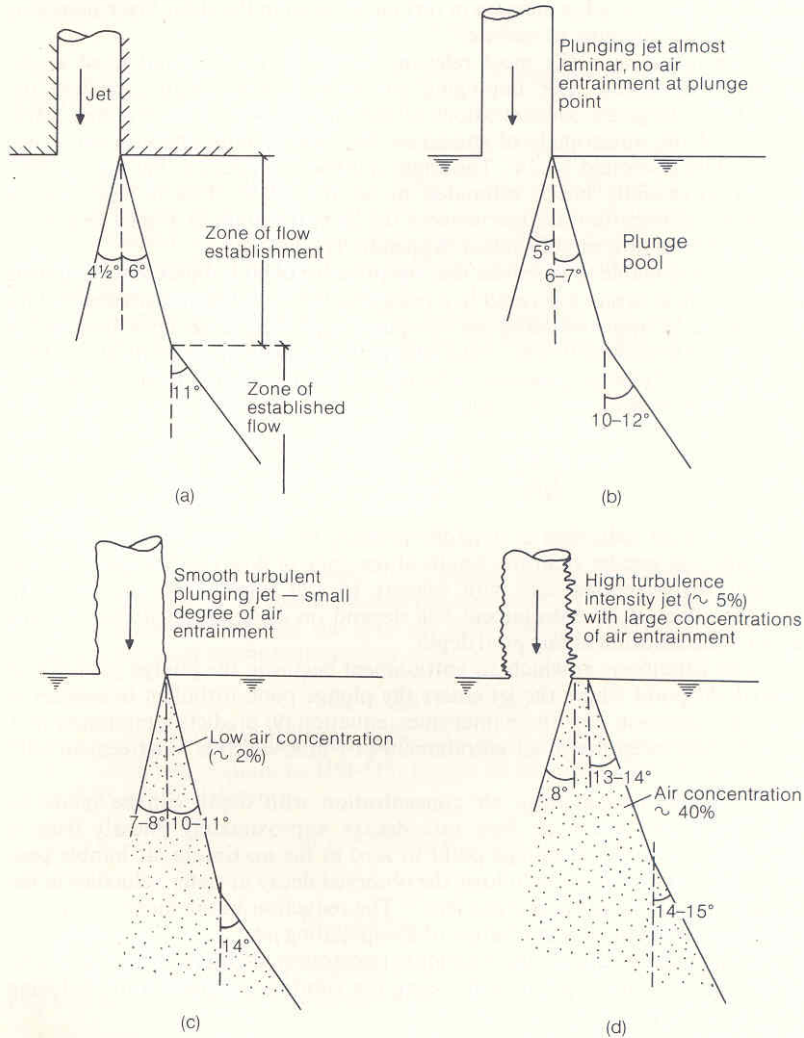


Figure 9. - Jet diffusion in a plunge pool for single-phase and two-phase shear layers: a) submerged jet ; b) almost laminar plunging jet; c) smooth turbulent plunging jet; d) highly turbulent plunging jet (Ervin and Falvey, 1987)

The core of the jet will dissipate or contract until the energy no longer remains to impact a surface and the outside of the jet will disperse. Both the core and outer diameter of the jet will change as a function of the incoming velocity and turbulence. It was assumed that the core would dissipate at an angle of 8 degrees as it falls through the tailwater. Performing the calculation determined that the core of the jet would be fully dissipated in

10 ft. Therefore, there will be no impact on the rock of the abutments in the tailwater pool below elevation 4660.

The outer edges of the jet will disperse at an angle of 6 to 14 degrees depending upon the initial turbulence level of the jet. The outer edge of the jet for Gibson Dam was assumed to disperse at an angle of 14 degrees. As the jet spreads, the extent of the impact zone on the rock abutment will increase. Table 7 shows the jet characteristics for the PMF overtopping at Gibson Dam both above and below the tailwater. Table 7 shows the jet characteristics to a vertical fall distance below the dam parapet wall of 215 ft, below the predicted foundation elevation at the toe of the dam.

Table 7. - Jet characteristics for the PMF overtopping of Gibson Dam including both the free-falling jet and the jet below the tailwater.

Vertical distance (y) from parapet elevation (ft)	Horizontal distance (x) from downstream parapet	Elevation of lower nappe (ft)	Elevation of upper nappe (ft)	Trajectory length (ft)	Velocity of jet at impact with various elevations. (ft/s)	Outer width of jet (ft)	Jet angle of impingement (degrees)
y (ft)	x (ft)	El. Under side	El. Upper nappe	ft	ft/s	ft	
0.00	0.00	4729.00	4736.43	0.00	40.18	7.43	0.00
-1.00	6.38	4728.00	4735.43	6.68	40.97	7.59	23.22
-2.00	9.02	4727.00	4734.43	9.87	41.75	7.66	31.24
-3.00	11.05	4726.00	4733.43	12.57	42.51	7.72	36.61
-4.00	12.75	4725.00	4732.43	15.06	43.27	7.78	40.63
-5.00	14.26	4724.00	4731.43	17.42	44.00	7.83	43.81
-10.00	20.17	4719.00	4726.43	28.40	47.52	8.08	53.60
-15.00	24.70	4714.00	4721.43	38.86	50.80	8.32	58.96
-20.00	28.52	4709.00	4716.43	49.13	53.87	8.55	62.47
-25.00	31.89	4704.00	4711.43	59.30	56.78	8.78	65.00
-30.00	34.93	4699.00	4706.43	69.43	59.55	9.02	66.95
-35.00	37.73	4694.00	4701.43	79.52	62.20	9.25	68.49
-40.00	40.33	4689.00	4696.43	89.59	64.73	9.48	69.77
-45.00	42.78	4684.00	4691.43	99.65	67.17	9.70	70.84
-50.00	45.09	4679.00	4686.43	109.70	69.53	9.93	71.75
-55.00	47.29	4674.00	4681.43	119.74	71.81	10.16	72.55
-59.00	48.98	4670.00	4677.43	127.76	73.58	10.35	73.12
-60.00	49.40	4669.00	4676.43	129.77	74.02	10.39	73.25
-65.00	51.41	4664.00	4671.43	139.80	76.16	10.62	73.87
-68.00	52.59	4661.00	4668.43	145.81	77.42	10.76	74.22
-69.00	52.97	4660.00	4667.43	147.82	77.83	10.80	74.32
-70.00	53.36	4659.00	4666.43	149.82	78.25	10.85	74.43
-75.00	55.23	4654.00	4661.43	159.84	80.28	11.08	74.94
-80.00	57.04	4649.00	4656.43	169.86	82.26	11.31	75.39
-85.00	58.79	4644.00	4651.43	179.88	84.19	11.53	75.81
-90.00	60.50	4639.00	4646.43	189.90	86.08	11.76	76.20
-95.00	62.16	4634.00	4641.43	199.91	87.93	11.99	76.55
-100.00	63.77	4629.00	4636.43	209.92	89.75	12.22	76.88

Gibson Dam Overtopping Investigations
4/12/2006

Vertical distance (y) from parapet elevation (ft)	Horizontal distance (x) from downstream parapet	Elevation of lower nappe (ft)	Elevation of upper nappe (ft)	Trajectory length (ft)	Velocity of jet at impact with various elevations. (ft/s)	Outer width of jet (ft)	Jet angle of impingement (degrees)
-105.00	65.35	4624.00	4631.43	219.93	91.52	12.45	77.18
-110.00	66.88	4619.00	4626.43	229.94	93.26	12.68	77.47
-115.00	68.39	4614.00	4621.43	239.95	94.98	12.90	77.74
-120.00	69.86	4609.00	4616.43	249.96	96.66	13.13	77.99
-125.00	71.30	4604.00	4611.43	259.97	98.31	13.36	78.22
-130.00	72.71	4599.00	4606.43	269.98	99.93	13.59	78.45
-135.00	74.10	4594.00	4601.43	279.98	101.53	13.82	78.66
-140.00	75.46	4589.00	4596.43	289.99	103.10	14.04	78.86
-145.00	76.79	4584.00	4591.43	299.99	104.65	14.27	79.04
-150.00	78.10	4579.00	4586.43	310.00	106.18	14.50	79.22
-155.00	79.39	4574.00	4581.43	320.01	107.69	14.73	79.40
-160.00	80.67	4569.00	4576.43	330.01	109.17	14.96	79.56
-165.00	81.92	4564.00	4571.43	340.02	110.64	15.18	79.71
-170.00	83.15	4559.00	4566.43	350.02	112.08	15.41	79.86
-175.00	84.36	4554.00	4561.43	360.02	113.51	15.64	80.01
-180.00	85.56	4549.00	4556.43	370.03	114.92	15.87	80.14
-185.00	86.74	4544.00	4551.43	380.03	116.31	16.10	80.28
-195.00	89.05	4534.00	4541.43	400.04	119.05	16.55	80.52
-200.00	90.19	4529.00	4536.43	410.04	120.39	16.78	80.64
-205.00	91.31	4524.00	4531.43	420.04	121.72	17.01	80.75
-210.00	92.41	4519.00	4526.43	430.05	123.04	17.24	80.86
-215.00	93.51	4514.00	4521.43	440.05	124.34	17.47	80.97

Shaded row indicates the location of the tailwater elevation at the PMF.

D. Stream Power

Figure 7 shows the predicted footprint of the jet at it would impinge on the rock or concrete overlay on the abutments. The concern is the pressure or force transmitted by the jet through either a very shallow depth of water below the tailwater, $Y/D_j < 4-6$, or where the impingement occurs above the tailwater. The pressures may be computed if necessary using results from Bollaert [19].

Once the jet characteristics have been defined the potential for scour may be determined. The scour potential may be quantified by determining the erosive stream power. The stream power is the rate at which energy is applied after the jet has travelled through a vertical distance, Z , to a location on a surface or in a pool.

$$P_{jet} = \gamma QZ$$

where P_{jet} is the total stream power of the jet, γ is the unit weight of water, and Q is the total discharge. The stream power per unit area is determined by dividing the total stream power by the footprint of the area of the jet at the point of impact. This stream power per unit area or stream power density of the jet is:

$$p_{jet} = \frac{\gamma QZ}{A_i}$$

and may be used to determine whether erosion will occur or not as a function of the erodibility of the material or rock. The unit area of the jet changes with the fall both above and below the tailwater. There is a limit or threshold of erosion based upon a body of empirical data.

The erodibility of the material that the jet impacts on is determined by analysis of many factors of the rock and is expressed as an erodibility index, K . The erodibility indices for the rock and concrete protection, shown in table 8, were determined for Gibson Dam by Elisabeth Cohen, Civil Engineer, D-8110, US Bureau of Reclamation, Technical Services Center [22].

A threshold of erodibility has been defined as a function of the erodibility index, K as follows [18]:

$$P_c = K^{0.75} \quad \text{for higher erodibility or } K > 0.1$$

$$P_c = 0.48K^{0.44} \quad \text{for less erodibility or } K < 0.1$$

The threshold stream power densities were computed for the K values for Gibson Dam and are also shown in table 8. Erosion will occur for conditions plotting above the P_c , or “erosion threshold line”, shown on the figure 10 of stream power density versus erodibility index.

Table 8. - Estimated erodibility indices and critical stream power values for the surface downstream from Gibson Dam.

Material	Erodibility Index (K)	Threshold Stream Power Density (kW/m ²) (P _c)
concrete - low	6400	715
concrete - high	8500	885
fractured rock – low	200	53
fractured rock – high	400	89
Hard foundation rock - low	5100	603
Hard foundation rock - high	12000	1146

Figure 10 also shows the between stream power densities and erodibility indices for the 1964 overtopping event of 18,000 ft³/s at Gibson Dam. The stream power was computed to be from 43 to 258 kW/m² at the upper and lower abutments, respectively, at a unit discharge of 19.2 cfs/ft. The fractured foundation material with lower erodibility showed some scour and the hard foundation material showed no scour.

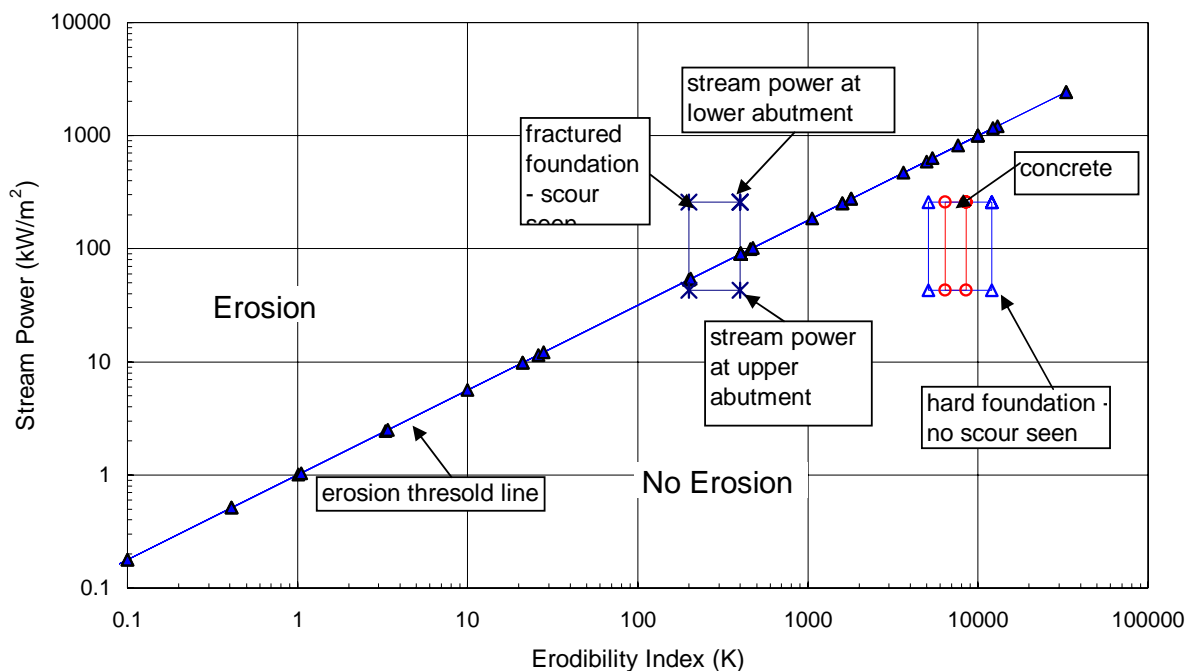


Figure 10. - Stream power versus erodibility index for the 1964 overtopping event at Gibson Dam.

The stream power was computed for the new PMF event of 182,580 ft³/s with the jet characteristics as determined in the previous sections. The stream power was computed both above and below the tailwater. The jet characteristics determined for entry to the pool and for dispersion in the pool are very important in the computation of the stream power. For this case, the core of the jet will dissipate through the pool and no longer produce additional impact after elevation 4660. At impact with the tailwater pool, the outer dimension of the jet has spread to 10.35 ft and will continue spreading through the pool, thus decreasing the stream power per unit area, as expected. The results of the stream power per unit area computations are shown in table 9 and figure 11. The tailwater

will be affected by the flow over the top of the dam, thus producing slightly different results.

Table 9. - Stream power in the flow and the width of the jet per unit area at various elevations at Gibson Dam.

El. Nappe under side	Area of jet footprint (ft ²)	Stream power density (ft-lb/s/ft)	Stream power density (ft-lb/s-ft ²)	Stream power density (HP/ft ²)	Stream power density (kW/m ²)
4729.00	7.43	176966	23809	43	347
4728.00	7.59	188843	24897	45	363
4727.00	7.66	200720	26212	48	383
4726.00	7.72	212597	27541	50	402
4725.00	7.78	224474	28868	52	421
4724.00	7.83	236351	30186	55	441
4719.00	8.08	295735	36600	67	534
4714.00	8.32	355120	42690	78	623
4709.00	8.55	414505	48465	88	707
4704.00	8.78	473889	53945	98	787
4699.00	9.02	533274	59150	108	863
4694.00	9.25	592659	64101	117	935
4689.00	9.48	652043	68815	125	1004
4684.00	9.70	711428	73308	133	1070
4679.00	9.93	770812	77596	141	1132
4674.00	10.16	830197	81691	149	1192
4670.00	10.35	877705	84838	154	1238
4669.00	10.70	889582	83152	151	1213
4664.00	12.46	948966	76152	138	1111
4661.00	13.52	984597	72828	132	1063
4660.00	13.87	996474	71833	131	1048
4659.00	14.22	1008351	70887	129	1035
4654.00	15.99	1067736	66783	121	975
4649.00	17.75	1127120	63495	115	927
4644.00	19.51	1186505	60801	111	887
4639.00	21.28	1245889	58553	106	855
4634.00	23.04	1305274	56650	103	827
4629.00	24.80	1364659	55017	100	803
4624.00	26.57	1424043	53601	97	782
4619.00	28.33	1483428	52361	95	764
4614.00	30.09	1542813	51266	93	748
4609.00	31.86	1602197	50293	91	734
4604.00	33.62	1661582	49421	90	721
4599.00	35.38	1720966	48637	88	710
4594.00	37.15	1780351	47927	87	699
4589.00	38.91	1839736	47281	86	690
4584.00	40.67	1899120	46691	85	681
4579.00	42.44	1958505	46151	84	674
4574.00	44.20	2017890	45653	83	666
4569.00	45.96	2077274	45194	82	660
4564.00	47.73	2136659	44768	81	653
4559.00	49.49	2196043	44373	81	648
4554.00	51.25	2255428	44005	80	642
4549.00	53.02	2314813	43662	79	637
4544.00	54.78	2374197	43341	79	632

Shaded row indicates the location of the tailwater elevation at the PMF.

Figure 11 shows that the stream power is high enough in the fractured rock zone for erosion to be predicted. Even in the hard foundation and concrete the available energy is enough for scour to be predicted.

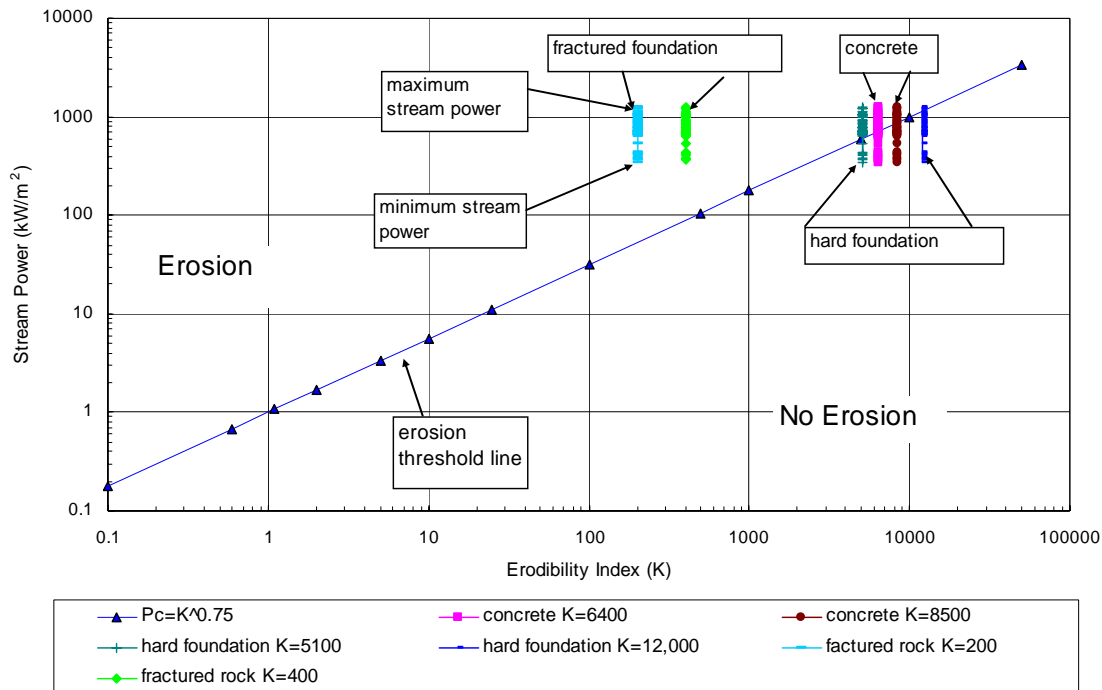


Figure 11. - Relationship between stream power and erodibility index for the PMF overtopping of Gibson Dam. Estimates shown include stream power above and below the tailwater.

The maximum stream power density of 154 HP/ft² or 1238 kw/m² occurs at the maximum drop from the dam to the abutments prior to the jet entering the tailwater pool.

X. Recommendations

The following recommendation is made as a result of this investigation into the hydraulic loading due to the PMF overtopping at Gibson Dam:

- Further investigate the abutment rock to determine if the fractured rock where flow impingement will occur may be sound enough.
- Determine with the client if the risk is acceptable to do nothing and note that the jet will impinge on the rock at the 100,000 year flood event.

XI. References

- [1] "Issue Evaluation Report of Findings," Gibson Dam, Sun River Project, Montana, Technical Service Center, Bureau of Reclamation, Denver, Colorado, May 2004.
- [2] "Gibson Dam, Comprehensive Facility Review," Sun River Project, Great Plains Region, Technical Service Center, Bureau of Reclamation, Denver, Colorado, December 2004.
- [3] "Gibson Dam, Montana, Hydrologic Hazard," Flood Hydrology Group, D-8530, Technical Service Center, Bureau of Reclamation, Denver, Colorado, September 2005.
- [4] "Gibson Dam Frequency Flood Routings for Corrective Action Study," Sun River Project, Great Plains Region, Technical Service Center, Bureau of Reclamation, Denver, Colorado, November 2005.
- [5] "Standing Operating Procedures, Gibson Dam and Reservoir," Sun River Project, Montana, Great Plains Region, Bureau of Reclamation, Department of the Interior, Copy No. 1L, February 2005.
- [6] "Hydraulic Model Studies For The Glory-Hole Spillways at Owyhee Dam – Owyhee Project, Oregon-Idaho, and Gibson Dam – Sun River Project, Montana," Hydraulic Laboratory Report No. HYD-159, Prepared by F.C. Lowe, Bureau of Reclamation, Denver, Colorado, November 15, 1944.
- [7] Memorandum to Files, from E.R. Anesi, Chief, Reservoir Regulation Branch, Subject: "Flood of June 8-9, 1964, on Sun River at Gibson Dam," September 22, 1964.
- [8] Calcagno Jr., Frank, "Geologic Report on the Modification of Gibson Dam," Bureau of Reclamation, Billings, Montana, May 1982.
- [9] Memorandum to Acting Assistant Commissioner from Chief, Division of Technical Review, Review of Design Summary for Gibson Dam Modifications, Bureau of Reclamation, Denver, Colorado, October 1980.
- [10] Travel Report, From David Allen and Mas Arai, To chief Design Engineer, and Chief, Division of Geology, Examination of the Concrete Cap and its Foundation at Gibson Dam, Bureau of Reclamation, Denver, Colorado, October 1980.
- [11] CFR November 2004
- [12] FLROUT (PC Version), Flood Routing Program [computer program], Bureau of Reclamation, Denver, Colorado, August 1993.

- [13] “Probable Maximum Flood Study for Gibson Dam, Montana, Using HMR 55A Probable Maximum Precipitation,” Flood Hydrology Group, Bureau of Reclamation, Denver, Colorado, July 20, 2005.
- [14] Notes by Bruce Feinberg, D-8540, providing tailwater information.
- [15] Rouse, H. R., 1936, “Discharge Characteristics of the Free Overfall,” Civil Engineering, Vol. 6, No. 4.
- [16] Lewis, T.M, Abt, S.R., Ruff, J.F., 1996, “Prediction of Velocities within Jets Formed by Overtopping Steep Dams,” Department of Civil Engineering, Colorado State University, Fort Collins, Colorado, March 1996.
- [17] Design of Small Dams, 3rd Edition, Bureau of Reclamation, United States Department of the Interior, United States Government Printing Office, Denver, Colorado, 1987.
- [18] Annandale, George W., 2006, “Scour Technology *Mechanics and Engineering Practice*,” McGraw-Hill Civil Engineering Series, ISBN 0-07-144057-7.
- [19] Bollaert, Erik, 2002, “Transient water pressures in joints and formation of rock scour due to high-velocity jet impact,” Communication 13, Laboratoire de Constructions Hydrauliques Ecole Polytechnique Federale de Lausanne, Edited by Professor Dr. A. Schleiss, Lausanne, Switzerland, 2002.
- [20] Ervine, D.A., et al, 1997, “Pressure Fluctuations on Plunge Pool Floors,” Journal of Hydraulic Research, Vol. 35, No. 2, pp. 257-279.
- [21] Ervine and Falvey, 1987, “Behaviour of turbulent water jets in the atmosphere and in plunge pools,” Proceedings Institution of Civil Engineers, Part 2, Volume 83, pp. 295-314.
- [22] Cohen, E. A., 1998, “Case History Summary, Gibson Dam,” DSO-98-005, US Department of the Interior, Bureau of Reclamation, Denver, CO.

Appendix A - Drawings of Gibson Dam Plan and Profile

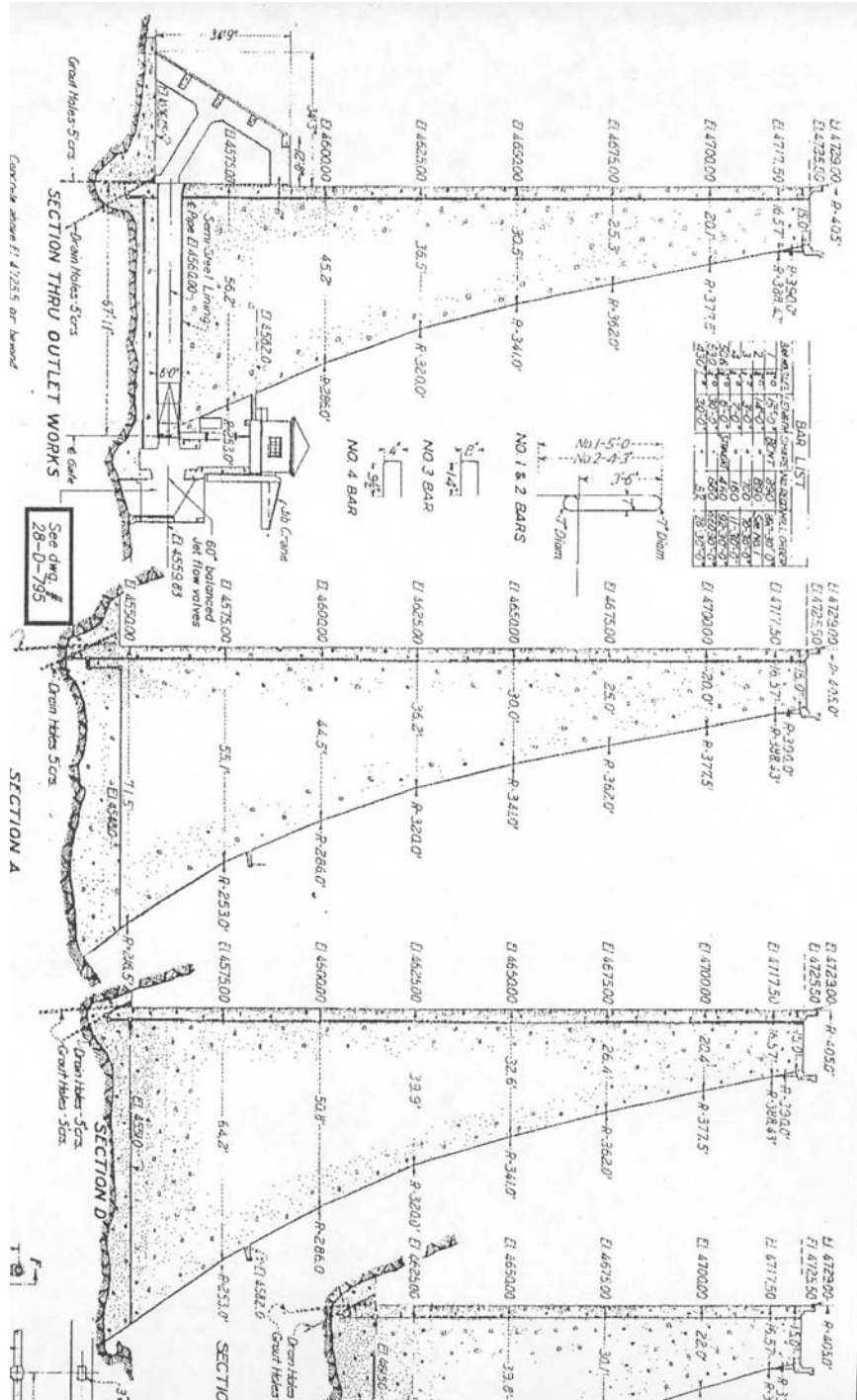


Figure 13. - Sections through Gibson Dam showing the top of dam and the overall extent of the dam section.

**Appendix B – Sensitivity of the jet trajectory to the “K” factor
in the equation of motion.**

y (ft)	k=1			k=0.9			k=0.75		
	x (ft)	El. Under side	El. Upper nappe	x (ft)	El. Under side	El. Upper nappe	x (ft)	El. Under side	El. Upper nappe
0.00	0.00	4729.00	4736.43	0.00	4729.00	4736.43	0.00	4729.00	4736.43
-1.00	6.38	4728.00	4735.43	6.05	4728.00	4735.43	5.52	4728.00	4735.43
-2.00	9.02	4727.00	4734.43	8.56	4727.00	4734.43	7.81	4727.00	4734.43
-3.00	11.05	4726.00	4733.43	10.48	4726.00	4733.43	9.57	4726.00	4733.43
-4.00	12.75	4725.00	4732.43	12.10	4725.00	4732.43	11.05	4725.00	4732.43
-5.00	14.26	4724.00	4731.43	13.53	4724.00	4731.43	12.35	4724.00	4731.43
-10.00	20.17	4719.00	4726.43	19.13	4719.00	4726.43	17.46	4719.00	4726.43
-15.00	24.70	4714.00	4721.43	23.43	4714.00	4721.43	21.39	4714.00	4721.43
-20.00	28.52	4709.00	4716.43	27.06	4709.00	4716.43	24.70	4709.00	4716.43
-25.00	31.89	4704.00	4711.43	30.25	4704.00	4711.43	27.61	4704.00	4711.43
-30.00	34.93	4699.00	4706.43	33.14	4699.00	4706.43	30.25	4699.00	4706.43
-35.00	37.73	4694.00	4701.43	35.79	4694.00	4701.43	32.67	4694.00	4701.43
-40.00	40.33	4689.00	4696.43	38.26	4689.00	4696.43	34.93	4689.00	4696.43
-45.00	42.78	4684.00	4691.43	40.58	4684.00	4691.43	37.05	4684.00	4691.43
-50.00	45.09	4679.00	4686.43	42.78	4679.00	4686.43	39.05	4679.00	4686.43
-55.00	47.29	4674.00	4681.43	44.87	4674.00	4681.43	40.96	4674.00	4681.43
-59.00	48.98	4670.00	4677.43	46.47	4670.00	4677.43	42.42	4670.00	4677.43
-60.00	49.40	4669.00	4676.43	46.86	4669.00	4676.43	42.78	4669.00	4676.43
-65.00	51.41	4664.00	4671.43	48.78	4664.00	4671.43	44.53	4664.00	4671.43
-68.00	52.59	4661.00	4668.43	49.89	4661.00	4668.43	45.54	4661.00	4668.43
-69.00	52.97	4660.00	4667.43	50.25	4660.00	4667.43	45.88	4660.00	4667.43
-70.00	53.36	4659.00	4666.43	50.62	4659.00	4666.43	46.21	4659.00	4666.43
-75.00	55.23	4654.00	4661.43	52.39	4654.00	4661.43	47.83	4654.00	4661.43
-80.00	57.04	4649.00	4656.43	54.11	4649.00	4656.43	49.40	4649.00	4656.43
-85.00	58.79	4644.00	4651.43	55.78	4644.00	4651.43	50.92	4644.00	4651.43
-90.00	60.50	4639.00	4646.43	57.39	4639.00	4646.43	52.39	4639.00	4646.43
-95.00	62.16	4634.00	4641.43	58.97	4634.00	4641.43	53.83	4634.00	4641.43
-100.00	63.77	4629.00	4636.43	60.50	4629.00	4636.43	55.23	4629.00	4636.43
-105.00	65.35	4624.00	4631.43	61.99	4624.00	4631.43	56.59	4624.00	4631.43
-110.00	66.88	4619.00	4626.43	63.45	4619.00	4626.43	57.92	4619.00	4626.43
-115.00	68.39	4614.00	4621.43	64.88	4614.00	4621.43	59.23	4614.00	4621.43
-120.00	69.86	4609.00	4616.43	66.27	4609.00	4616.43	60.50	4609.00	4616.43
-125.00	71.30	4604.00	4611.43	67.64	4604.00	4611.43	61.75	4604.00	4611.43
-130.00	72.71	4599.00	4606.43	68.98	4599.00	4606.43	62.97	4599.00	4606.43
-135.00	74.10	4594.00	4601.43	70.29	4594.00	4601.43	64.17	4594.00	4601.43
-140.00	75.46	4589.00	4596.43	71.58	4589.00	4596.43	65.35	4589.00	4596.43
-145.00	76.79	4584.00	4591.43	72.85	4584.00	4591.43	66.50	4584.00	4591.43
-150.00	78.10	4579.00	4586.43	74.10	4579.00	4586.43	67.64	4579.00	4586.43
-155.00	79.39	4574.00	4581.43	75.32	4574.00	4581.43	68.76	4574.00	4581.43
-160.00	80.67	4569.00	4576.43	76.53	4569.00	4576.43	69.86	4569.00	4576.43
-165.00	81.92	4564.00	4571.43	77.71	4564.00	4571.43	70.94	4564.00	4571.43
-170.00	83.15	4559.00	4566.43	78.88	4559.00	4566.43	72.01	4559.00	4566.43
-175.00	84.36	4554.00	4561.43	80.03	4554.00	4561.43	73.06	4554.00	4561.43
-180.00	85.56	4549.00	4556.43	81.17	4549.00	4556.43	74.10	4549.00	4556.43
-185.00	86.74	4544.00	4551.43	82.29	4544.00	4551.43	75.12	4544.00	4551.43

Table 9. - Table of computed jet trajectories for various K values for the PMF overtopping of Gibson Dam.

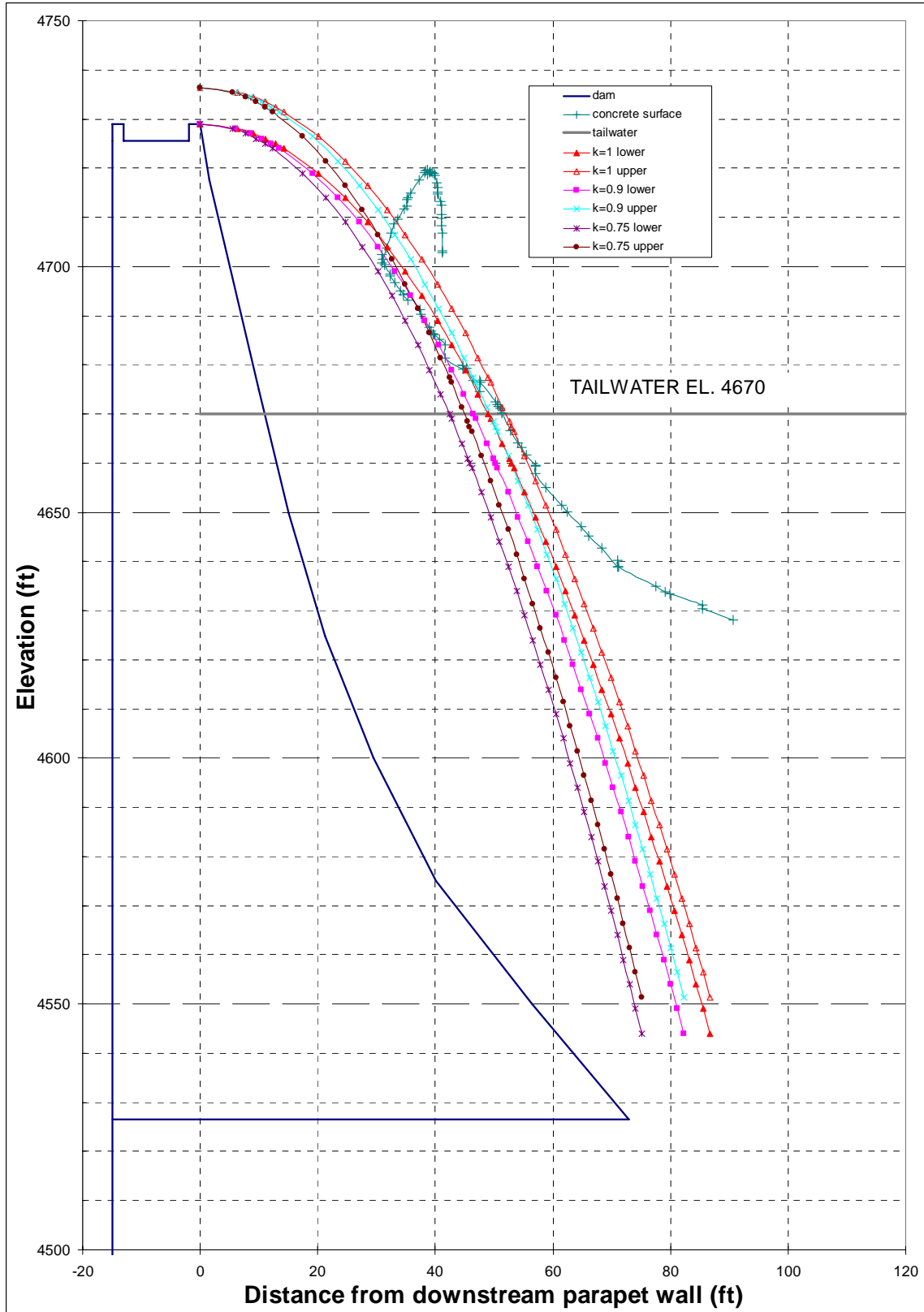


Figure 14. - Comparison of jet trajectories with the assumed K factor for the PMF overtopping of Gibson Dam.